NASA/TM-20205008464

# Effect of Ram and Zenith Exposure on the Optical Properties of Polymers in Space

*Yuanchun Li*
*Hathaway Brown School, Shaker Heights, Ohio*

*Kim K. de Groh*
*Glenn Research Center, Cleveland, Ohio*

*Bruce A. Banks*
*Science Applications International Corporation, Cleveland, Ohio*

*Halle A. Leneghan and Olivia C. Asmar*
*Hathaway Brown School, Shaker Heights, Ohio*

*Henry C. de Groh III*
*Glenn Research Center, Cleveland, Ohio*

December 2020

# NASA STI Program . . . in Profile

Since its founding, NASA has been dedicated to the advancement of aeronautics and space science. The NASA Scientific and Technical Information (STI) Program plays a key part in helping NASA maintain this important role.

The NASA STI Program operates under the auspices of the Agency Chief Information Officer. It collects, organizes, provides for archiving, and disseminates NASA's STI. The NASA STI Program provides access to the NASA Technical Report Server—Registered (NTRS Reg) and NASA Technical Report Server—Public (NTRS) thus providing one of the largest collections of aeronautical and space science STI in the world. Results are published in both non-NASA channels and by NASA in the NASA STI Report Series, which includes the following report types:

- TECHNICAL PUBLICATION. Reports of completed research or a major significant phase of research that present the results of NASA programs and include extensive data or theoretical analysis. Includes compilations of significant scientific and technical data and information deemed to be of continuing reference value. NASA counter-part of peer-reviewed formal professional papers, but has less stringent limitations on manuscript length and extent of graphic presentations.

- TECHNICAL MEMORANDUM. Scientific and technical findings that are preliminary or of specialized interest, e.g., "quick-release" reports, working papers, and bibliographies that contain minimal annotation. Does not contain extensive analysis.

- CONTRACTOR REPORT. Scientific and technical findings by NASA-sponsored contractors and grantees.

- CONFERENCE PUBLICATION. Collected papers from scientific and technical conferences, symposia, seminars, or other meetings sponsored or co-sponsored by NASA.

- SPECIAL PUBLICATION. Scientific, technical, or historical information from NASA programs, projects, and missions, often concerned with subjects having substantial public interest.

- TECHNICAL TRANSLATION. English-language translations of foreign scientific and technical material pertinent to NASA's mission.

For more information about the NASA STI program, see the following:

- Access the NASA STI program home page at http://www.sti.nasa.gov

- E-mail your question to help@sti.nasa.gov

- Fax your question to the NASA STI Information Desk at 757-864-6500

- Telephone the NASA STI Information Desk at 757-864-9658

- Write to:
  NASA STI Program
  Mail Stop 148
  NASA Langley Research Center
  Hampton, VA 23681-2199

NASA/TM-20205008464

# Effect of Ram and Zenith Exposure on the Optical Properties of Polymers in Space

*Yuanchun Li*
*Hathaway Brown School, Shaker Heights, Ohio*

*Kim K. de Groh*
*Glenn Research Center, Cleveland, Ohio*

*Bruce A. Banks*
*Science Applications International Corporation, Cleveland, Ohio*

*Halle A. Leneghan and Olivia C. Asmar*
*Hathaway Brown School, Shaker Heights, Ohio*

*Henry C. de Groh III*
*Glenn Research Center, Cleveland, Ohio*

Prepared for the
2017 International Space Station Research and Development Conference (ISSRDC)
sponsored by the American Astronautical Society (AAS) with the support of the
Center for the Advancement of Science in Space (CASIS) and NASA
Washington D.C., July 17–20, 2017

National Aeronautics and
Space Administration

Glenn Research Center
Cleveland, Ohio 44135

December 2020

## Acknowledgments

We would like to express our sincere appreciation to Sharon Miller of NASA Glenn Research Center for providing oversight and assistance with the optical properties measurements over multiple years. We are also grateful to the Naval Research Laboratory and Gary Pippin, (retired) Boeing, for providing the opportunity to fly these experiments as part of the MISSE 7 mission. We would like to thank Patty Hunt (retired) and Dr. Crystal Miller of Hathaway Brown School (HB) for their support of the NASA Glenn Research Center and HB collaboration. This research was supported by the ISS Research Program, the MISSE-X Project, the MISSE Informatics Project and the Space Life and Physical Sciences Research and Applications (SPLSRA) Division.



*Level of Review*: This material has been technically reviewed by technical management.

Available from

NASA STI Program
Mail Stop 148
NASA Langley Research Center
Hampton, VA 23681-2199

National Technical Information Service
5285 Port Royal Road
Springfield, VA 22161
703-605-6000

This report is available in electronic form at http://www.sti.nasa.gov/ and http://ntrs.nasa.gov/

# Effect of Ram and Zenith Exposure on the Optical Properties of Polymers in Space

Yuanchun Li
Hathaway Brown School
Shaker Heights, Ohio 44122

Kim K. de Groh
National Aeronautics and Space Administration
Glenn Research Center
Cleveland, Ohio 44135

Bruce A. Banks
Science Applications International Corporation
Cleveland, Ohio 44135

Halle A. Leneghan and Olivia C. Asmar
Hathaway Brown School
Shaker Heights, Ohio 44122

Henry C. de Groh III
National Aeronautics and Space Administration
Glenn Research Center
Cleveland, Ohio 44135

**Abstract**

The temperature of spacecraft is influenced by the solar absorptance and thermal emittance of the external spacecraft materials in addition to heat generated within the spacecraft. Optical and thermal properties can degrade in the low Earth orbital (LEO) space environment where spacecraft external materials are exposed to various forms of radiation, thermal cycling, and atomic oxygen. One objective of the Polymers and Zenith Polymers Experiments was to determine the effect of LEO space exposure on the optical properties of various spacecraft polymers. These experiments were flown as part of the Materials International Space Station Experiment 7 (MISSE 7) mission on the exterior of the International Space Station (ISS) for1.5 years. Samples were flown in ram, wake and zenith directions, receiving varying amounts of atomic oxygen and solar radiation. Total and diffuse reflectance, and transmittance, of flight and corresponding control samples were obtained using a Cary 5000 UV-Vis-NIR Spectrophotometer. Integrated air mass zero solar absorptance ($\alpha_s$) of the flight and control ram and zenith samples were computed and compared. Optical and atomic oxygen erosion data are compared with similar MISSE 2 polymers exposed to space for four years. Results show that prolonged space exposure increases the solar absorptance of some materials. Knowing which polymers remain stable will benefit future spacecraft design.

## Introduction

The temperature of spacecraft is influenced by the solar absorptance ($\alpha_s$) and thermal emittance ($\varepsilon$) of the external spacecraft materials. Optical and thermal properties can degrade over time in the harsh low Earth orbit (LEO) space environment where spacecraft external materials are exposed to various forms of radiation, thermal cycling, and atomic oxygen (AO).[1] Each of these environmental exposures can cause degradation to spacecraft exterior polymeric components, and combined effects can cause even greater degradation. Changes in optical and thermal properties can negatively affect the temperature of the spacecraft leading to overheating or temperature drops. This can pose a threat to the efficiency and functionality of the spacecraft.

One of the biggest threats in the LEO space environment to exterior spacecraft polymers is AO erosion. Atomic oxygen is formed through photodissociation of molecular oxygen by short-wavelength ultraviolet (UV) radiation (>5.12 eV, <243 nm) from the sun.[2] In LEO, between the altitudes of 180 and 650 km, AO is the most abundant species.[1] For most polymers reacting with AO, the oxidation product is a gas such as CO or $CO_2$, therefore the material can literally erode away over time with AO exposure. The erosion of a material can be characterized by the material's AO erosion yield ($E_y$), which is the volume lost per incident oxygen atom ($cm^3$/atom).[1]

Another threat in the LEO space environment is UV radiation. Ultraviolet radiation has a typical wavelength of 0.1 to 0.4 micrometers[3]; these wavelengths are energetic enough to cause the breaking of organic bonds such as C = C, C = O, and C-H as well as other functional groups.[4] Molecules absorb energy when exposed to UV radiation. If the molecules acquire enough energy, bond dissociation can occur. Often UV radiation can cause color changes in polymers which can also affect the optical properties and functionality of the polymers.

It is important to test the durability of spacecraft materials in the space environment to ensure the most durable materials are being used to build spacecraft. A series of polymers experiments have been flown by NASA Glenn Research Center as part of the Materials International Space Station Experiment (MISSE) missions to determine the durability of polymers after LEO space exposure. In the MISSE 1-8 missions, individual experiments were loaded in flight trays called Passive Experiment Containers (PECs) and flown in either a ram/wake orientation or a zenith/nadir orientation on the exterior of the International Space Station (ISS).[5] A diagram showing ram, wake, zenith, and nadir directions on the ISS is shown in Figure 1. The flight orientation highly affects the environmental exposure. Ram facing experiments receive a high flux of directed AO and sweeping (moderate) solar exposure. Zenith facing experiments receive a low flux of grazing arrival AO and the highest solar exposure. Wake experiments receive very low AO flux and moderate solar radiation levels similar to ram experiments. Nadir experiments receive a low flux of grazing arrival AO and minimal solar radiation (albedo sunlight). All surfaces receive charged particle and cosmic radiation, which are omni-directional.

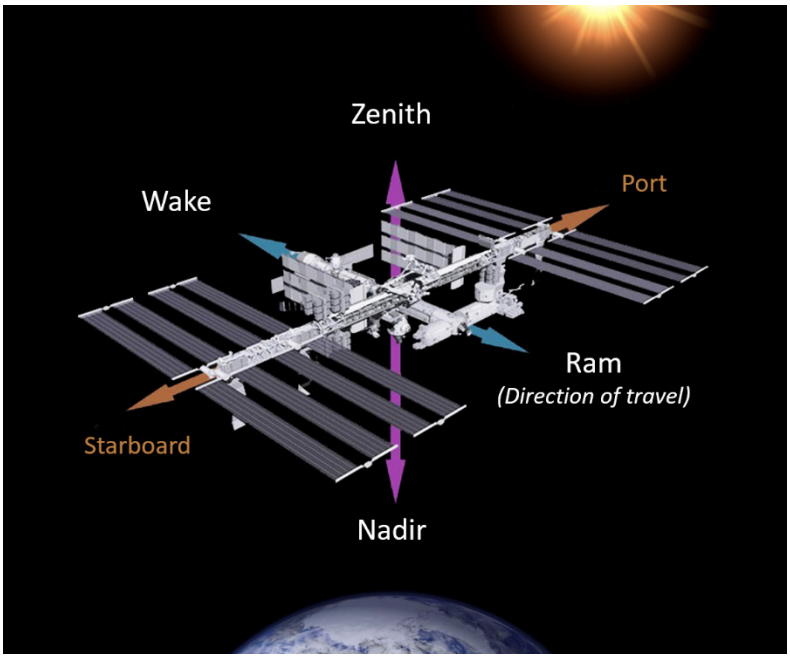


*Figure 1. Diagram showing ram (flight direction), wake, zenith, and nadir orientations on the International Space Station.*

As part of the MISSE 7 mission, two NASA Glenn Research Center experiments called the Polymers Experiment and the Zenith Polymers Experiment were flown on the exterior of the ISS and exposed to the LEO space environment for 1.5 years. Fifteen zenith samples from the Zenith Polymers Experiment and seven ram samples from the Polymers Experiment were characterized for changes in their optical properties. Wake samples were also flown however these 0.75" x 0.75" samples were too small for optical property measurements using our equipment, so they are not included here. The AO erosion yield of these MISSE 7 ram, wake, and zenith samples are presented in reference 1. As indicated above, changes in optical properties can pose a threat for the efficiency and functionality of the spacecraft. This paper provides an overview of the MISSE 7 mission, a description of the MISSE 7 Polymers Experiment and MISSE 7 Zenith Polymers Experiment with details on the samples characterized, the optical characterization technique, the AO fluence for the exposure orientations, and a summary of the optical property results. The optical data are compared with similar polymers exposed to space for four years as part of the MISSE 2 mission, and with AO erosion data, to help understand the degradation of these polymers in the space environment.

## Materials International Space Station Experiment (MISSE) Overview

The MISSE missions are a series of experiments that were flown on the exterior of the ISS to test the durability of materials in the LEO space environment. Individual flight experiments were flown in suitcase-like containers called Passive Experiment Containers (PECs) that provided exposure to the space environment. The PECs were closed during launch to protect the samples. Once on orbit, the PECs were placed on the exterior of the ISS during an extravehicular activity (EVA), or spacewalk, in either a ram/wake or zenith/nadir orientation and opened exposing the experiments to the space environment for the duration of the mission.

The MISSE 7 mission consisted of two PECs called MISSE 7A and 7B, which were flown in zenith/nadir and ram/wake orientations, respectively, on the ISS EXPRESS Logistic Carrier 2 (ELC-2) site. MISSE 7A and 7B were placed on the exterior of the ISS during the STS-129 Shuttle mission on November 23, 2009 and retrieved during the STS-134 Shuttle mission on May 20, 2011 after 1.49 years of space exposure. Figure 2 shows the location of MISSEs 7A and 7B on the ISS ELC-2. Figure 3 shows the zenith side of MISSE 7A and the ram side of 7B as imaged during the STS-130 mission in February 2010.

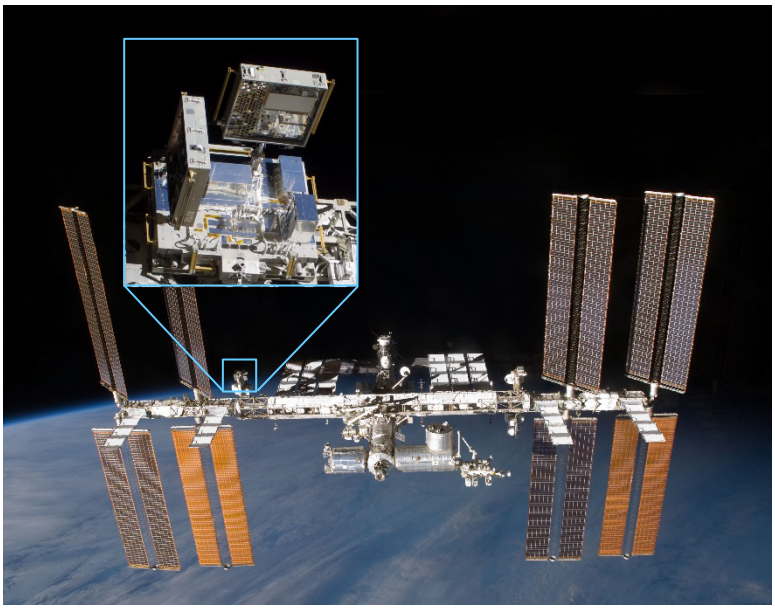

*Figure 2. Location of MISSEs 7A and 7B on the ISS ELC-2 as imaged during the STS-129 shuttle mission in November 2009 shortly after deployment.*

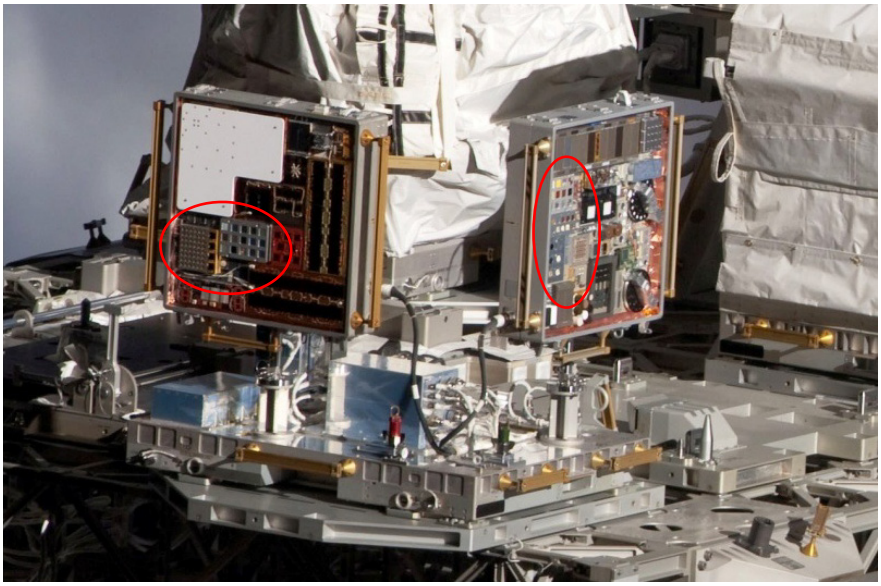

*Figure 3. MISSE7A (left) and MISSE 7B (right) on the International Space Station with the Zenith Polymers Experiment and Polymer Experiment samples circled in red.*[1]

### *MISSE 7B Polymers Experiment*

NASA Glenn's MISSE 7 Polymers Experiment was a passive experiment with 38 samples flown in the ram flight orientation and seven samples flown in the wake orientation on the MISSE 7B PEC.[1] Two of the objectives of this experiment were: 1.) To determine the LEO atomic oxygen erosion yield ($E_y$) of the polymers, and 2.) To assess the changes in optical properties of the polymers. The majority of samples were flown in two trays: Tray B7-R which held 15 - 1" (2.54 cm) square samples, shown in Figure 4, and Tray N5-R which held 16 - 0.75" (1.905 cm) square samples. In addition, numerous samples were flown in hand-made Al foil holders which were taped directly to the baseplate using thermal control tape. Pre- and post-flight photographs of the ram facing taped samples are shown in Figure 5a and Figure 5b, respectively. Kapton H, which has a well characterized AO $E_y$ of 3.0 x $10^{-24}$ $cm^3$/atom for LEO 4.5-eV AO[6-9], was flown in both the ram and wake directions for AO fluence determination in each flight orientation.

Table 1 provides a list of the seven MISSE 7B Polymers Experiment ram samples scanned and analyzed for changes in optical properties. There were five samples from tray B7-R and two taped samples (E13 and E14). One layer of each sample, along with one layer of the corresponding control sample were scanned. Descriptions of additional samples flown, along with the LEO AO erosion data are provided by de Groh in reference 1. Four MISSE 7 samples that were large enough to obtain optical properties (E17 (polyethylene oxide), E19 (120FG/EX1515 fiber glass/fiber/cyanate ester), E20 (M55J/954-3 carbon fiber/cyanate ester) and E21 (M55J/996 carbon fiber/cyanate ester) were not scanned because they did not have corresponding control samples.

Two white Tedlar samples (B7-2 and B7-3) were flown with different thicknesses of a temporary sacrificial Kapton H cover to lower the total mission AO fluence for those samples. Before the Kapton H erodes away, it protects the White Tedlar samples from AO erosion. White Tedlar sample B7-2 had a 0.5 mil (0.00127 cm) Kapton H cover. Based on a Kapton H LEO $E_y$ of 3.0 x $10^{-24}$ atoms/$cm^2$ from references 6-9, it takes an AO fluence of 4.23 x $10^{20}$ atoms/$cm^2$ to erode 0.5 mil of Kapton H. White Tedlar sample B7-3 had a 1.0 mil (0.00254 cm) Kapton H cover. It takes an AO fluence of 8.47 x $10^{20}$ atoms/$cm^2$ to erode 1.0 mil of Kapton H. This same technique has been used on MISSE 2 and MISSE 4 experiments each to control the amount of AO exposure of four DC 93-500 silicone samples.[10]

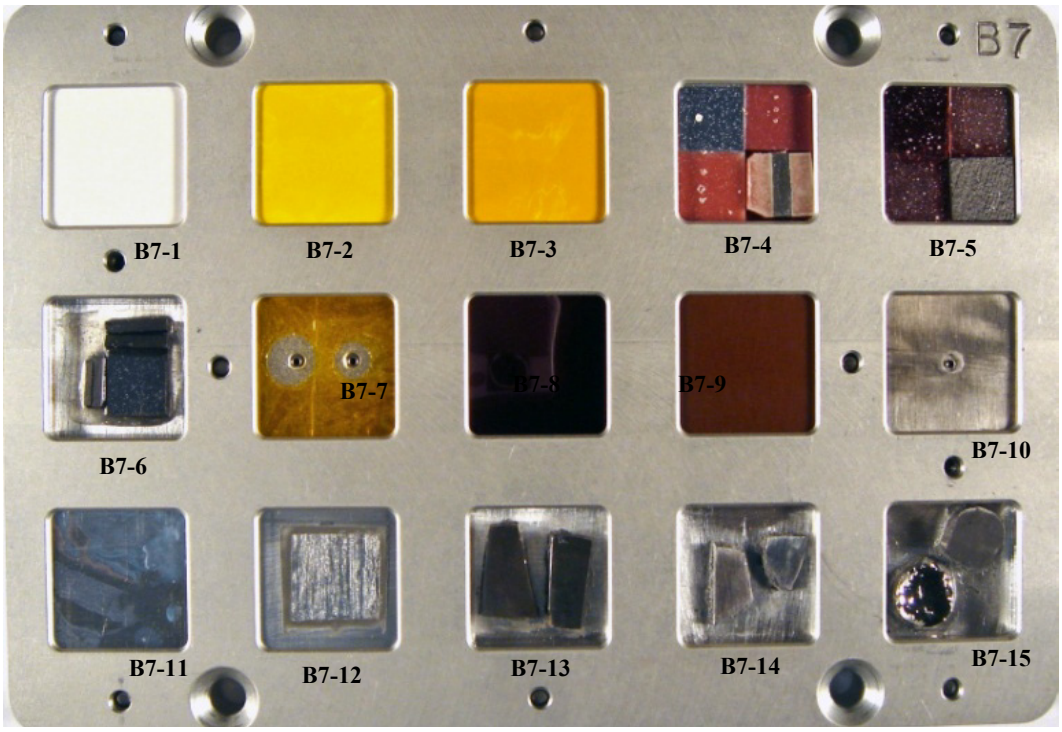


a.

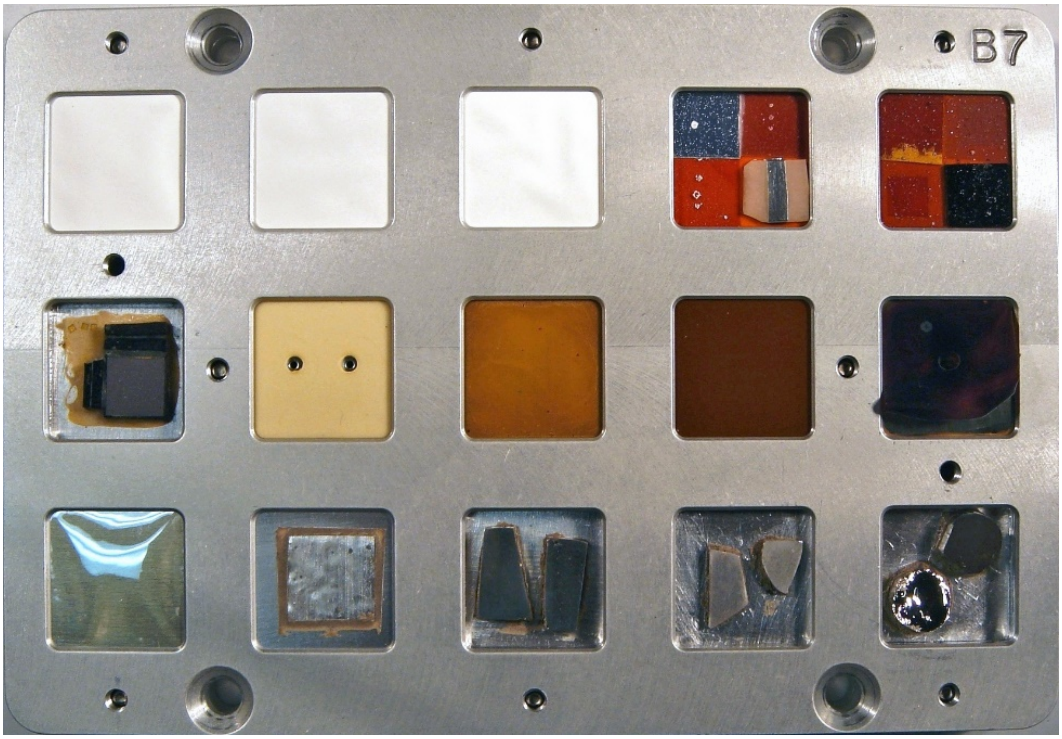


b.

*Figure 4. The MISSE 7 B7-R tray: a). Pre-flight photograph with sample IDs, and b). Post-flight photograph showing visual changes of numerous samples.*

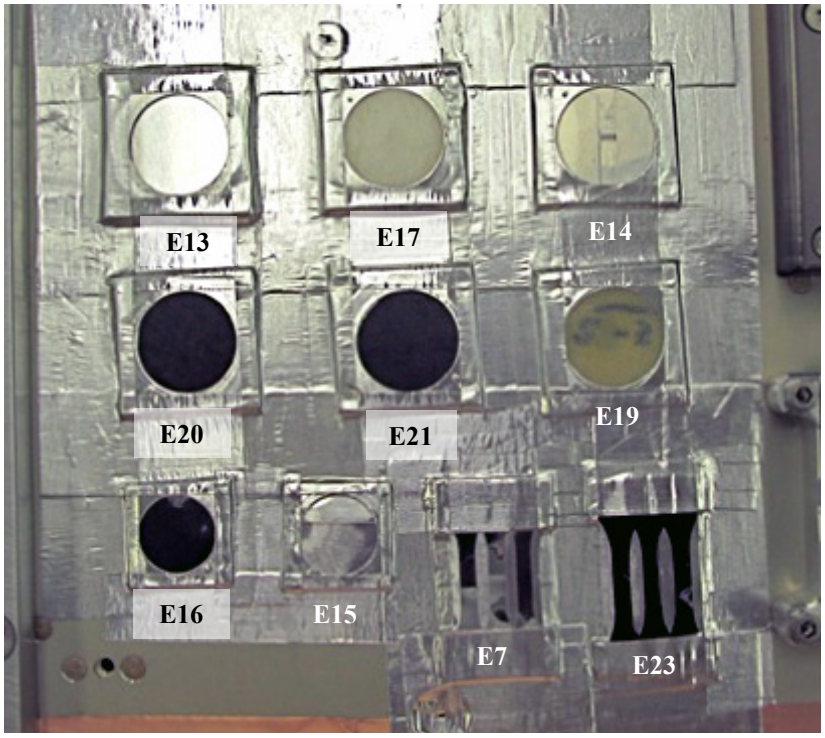


a.

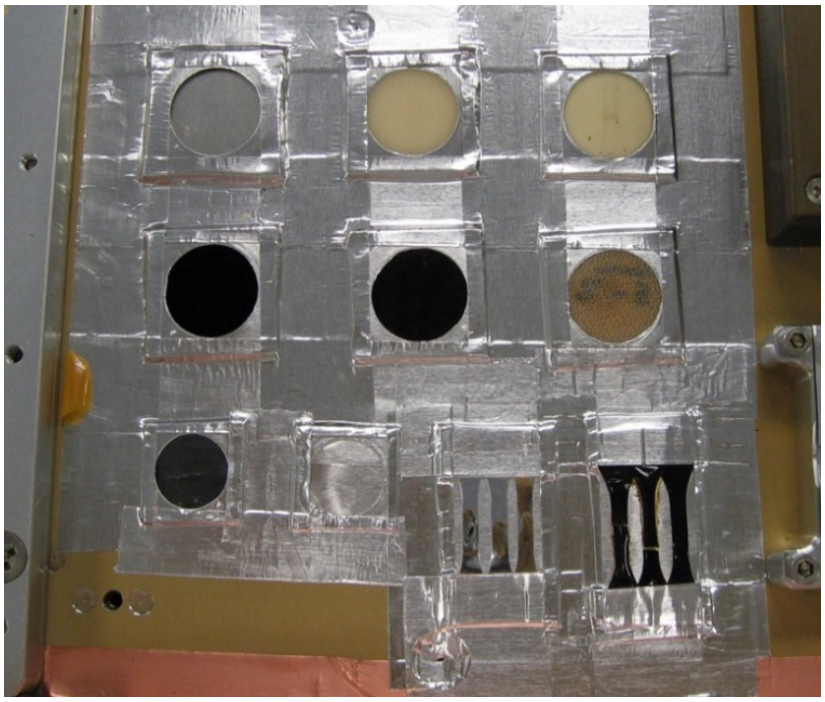

b.

*Figure 5. The MISSE 7B ram taped samples: a). Pre-flight photograph with samples IDs (courtesy of NRL), and b). Post-flight photograph showing darkening of some samples.*

Table 1. MISSE 7 Polymers Experiment Ram Optical Properties Samples.

| MISSE Sample ID | Material | Trade Name (Abbreviation) | Size (inches) | Thickness (mils) | # Layers Scanned/# Layers Flown |
|---|---|---|---|---|---|
| B7-1 | Crystalline polyvinyl fluoride w/ white pigment | White Tedlar (W-PVF) | 1 x 1 | 2 | 1/1 |
| B7-2 | Crystalline polyvinyl fluoride w/ white pigment with a 0.5 mil Kapton H cover | Kapton H/white Tedlar (W-PVF) | 1 x 1 | 2 | 1/1 |
| B7-3 | Crystalline polyvinyl fluoride w/ white pigment with two 0.5 mil Kapton covers (1.0 mil) | Kapton H/White Tedlar (W-PVF) | 1 x 1 | 2 | 1/1 |
| B7-8 | Polyimide (PMDA) | Kapton H (PI) | 1 x 1 | 5 | 1/4 |
| B7-9 | Polyimide | Vespel | 1 x 1 | 19.7 | 1/1 |
| E13 | $Al_2O_3$ Contamination Slide | ($Al_2O_3$) | 1" dia. | 625 | 1/1 |
| E14 | Polypropylene | (PP) | 1 x 1 | 20 | 1/1 |

### *MISSE 7A Zenith Polymers Experiment*

Glenn's MISSE 7 Zenith Polymers Experiment was a passive experiment with 25 samples in the zenith orientation on the MISSE 7A PEC.[1] Two of the objectives of the Zenith Polymers Experiment were: 1) to determine the effect of solar exposure on the $E_y$ of fluoropolymers under high solar/low AO exposure, and 2) to assess changes in optical properties of polymers exposed to zenith exposure. The experiment included 15 square samples, 1"x1" (2.54 $cm^2$), flown in the MISSE 7A "Z" tray. The Zenith Polymers Experiment also included 10 "taped" samples, flown in aluminum holders which were taped directly to the baseplate (similar to the ram and wake taped samples). Pre-flight and post-flight photographs of the Zenith Polymers Experiment Z tray is shown in Figure 6a and Figure 6b, respectively. The post-flight photograph shows substantial darkening of numerous polymers as compared to the pre-flight photograph. A pre-flight photograph of the zenith taped samples is provided in Figure 7. Table 2 provides a list of the 15 MISSE 7A Zenith Polymers Experiment samples scanned and analyzed for changes in optical properties. A Kapton H sample (Z-8) was flown for AO fluence determination in the zenith direction.

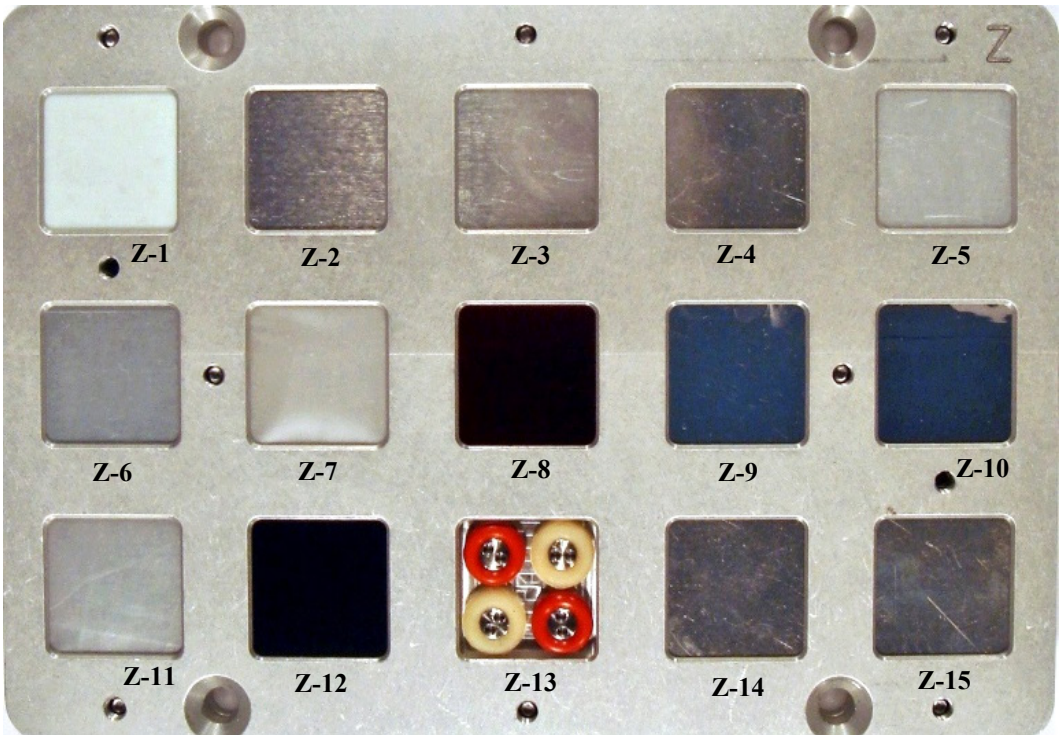


a.

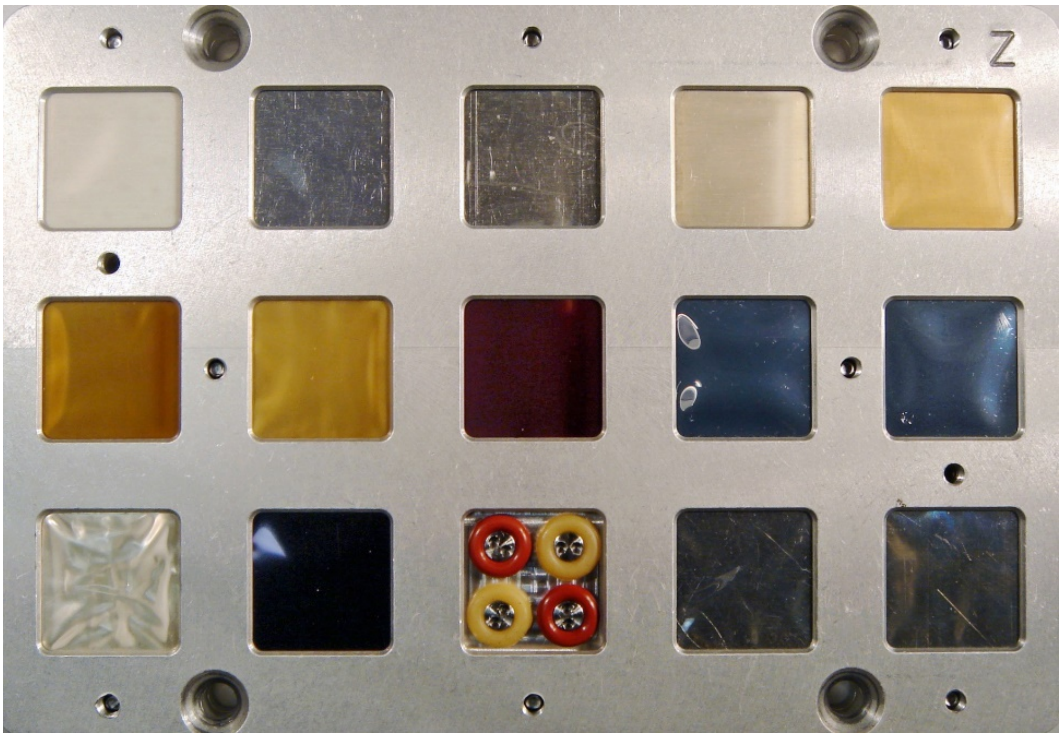


b.

*Figure 6. Photographs of the MISSE 7A Zenith Z tray: a). Pre-flight photograph with sample IDs, and b). Post-flight photograph showing darkening of numerous samples.*

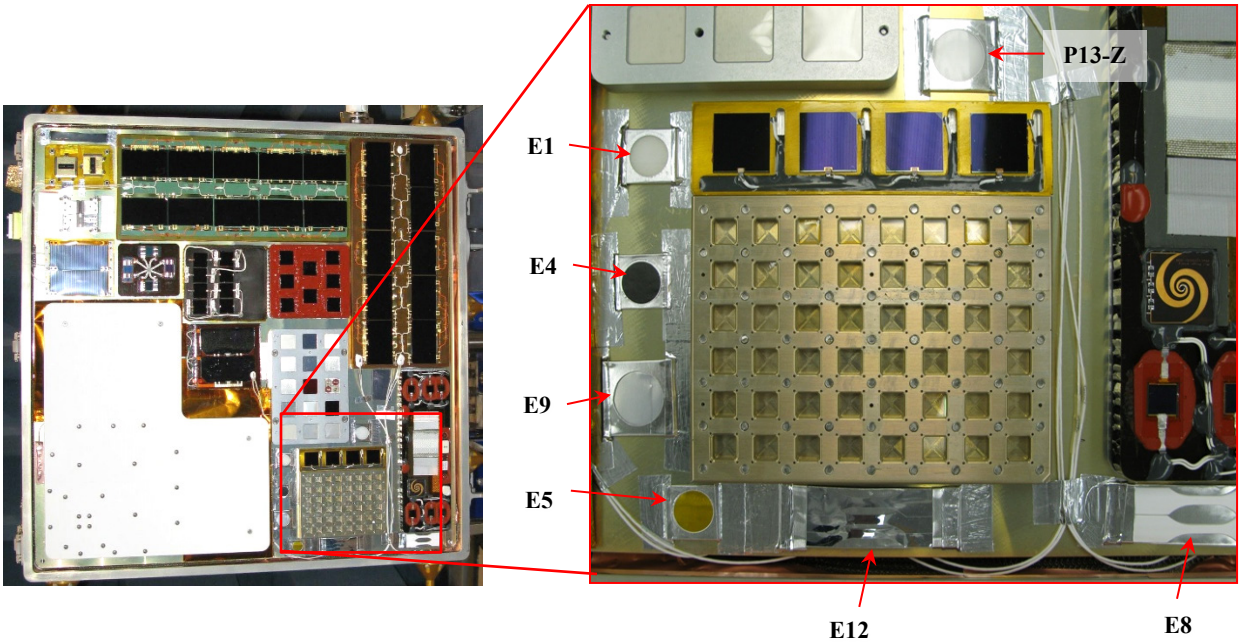


*Figure 7. Pre-flight photographs of the MISSE 7A zenith PEC with a close-up image of the taped samples with their sample IDs. (Photos courtesy of the Naval Research Laboratory)*

Table 2. MISSE 7 Zenith Experiment Optical Properties Samples.

| MISSE Sample ID | Material | Trade Name (Abbreviation) | Size (inches) | Polymer Thickness (mils) | # Layers Scanned/# Layers Flown |
|---|---|---|---|---|---|
| Z-1 | Polytetrafluoroethylene | Chemfilm DF-100 (PTFE) | 1 x 1 | 5 | 1/1 |
| Z-2 | Fluorinated ethylene propylene | Teflon (FEP) | 1 x 1 | 5 | 1/1 |
| Z-3 | Chlorotrifluoroethylene | Kel-F (CTFE) | 1 x 1 | 5 | 2/2 |
| Z-4 | Ethylene-tetrafluoroethylene copolymer | Tefzel ZM (ETFE) | 1 x 1 | 3 | 2/2 |
| Z-5 | Polyvinylidene fluoride | Kynar 740 (PVDF) | 1 x 1 | 3 | 1/2 & 2/2 |
| Z-6 | Ethylene-chlorotrifluoroethylene | Halar 300 (ECTFE) | 1 x 1 | 3 | 1/3 & 3/3 |
| Z-7 | Polyvinyl fluoride | Clear Tedlar (PVF) | 1 x 1 | 1 | 12/12 |
| Z-8 | Polyimide (PMDA) | Kapton H (PI) | 1 x 1 | 5 | 3/3 |
| Z-9 | Aluminized-fluorinated ethylene propylene* | Al-Teflon (Al-FEP) | 1 x 1 | 5 | 1/1 |
| Z-10 | Silvered-fluorinated ethylene propylene* | Ag-Teflon (Ag-FEP) | 1 x 1 | 5 | 1/1 |
| Z-11 | Polyethylene (low oxygen) | (PE) | 1 x 1 | 2 | 8/8 |
| Z-12 | Si/Kapton E/vapor deposited aluminium | (Si/Kapton E/VDA) | 1 x 1 | 2 | 1/1 |
| Z-14 | $Al_2O_3$/FEP | ($Al_2O_3$/FEP) | 1 x 1 | 2 | 1/1 |
| E9 | Polypropylene | (PP) | 1 x 1 | 20 | 1/1 |
| P13-Z | Polyvinyl alcohol | (PVOH) | 1 x 1 | 1.5 | 6/12 |

*Teflon layer was space facing

### *MISSE 7 Environment Exposure*

Table 3 lists the amount of solar exposure provided in equivalent sun hours (ESH) and the AO fluence the MISSE 7 polymers received in both the ram and zenith orientations.[1] Because the white Tedlar samples (B7-2 and B7-3) had sacrificial Kapton H covers, these two samples received different amounts of AO fluence and solar exposure due to the different thicknesses of the covers. The thicker the layer of Kapton H, the less AO fluence the white Tedlar sample received as indicted by the AO fluence listed in Table 3. The exposure of UV radiation for the white Tedlar samples flown with 0.5 and 1.0 mil Kapton H covers (2,150 ESH and 1,920 ESH, respectively) was estimated based on their time uncovered; their fractions uncovered were estimated by their AO fluence ratio relative to full ram exposure.

Table 3. AO Fluence and Solar Exposure of MISSE 7 Polymers.[1]

| MISSE 7 Orientations | Solar Exposure (ESH) | AO Fluence (atoms/cm$^2$) |
|---|---|---|
| Ram | 2,400 | $4.22\times10^{21}$ |
| Ram: B7-2 white Tedlar w/ 0.5 mil Kapton H | 2,150 | $3.79\times10^{21}$ |
| Ram: B7-3 white Tedlar w/ 1.0 mil Kapton H | 1,920 | $3.37\times10^{21}$ |
| Zenith | 4,300 | $1.58\times10^{20}$ |

## Experimental Procedures

### *Pre-flight Fabrication and Characterization*

The polymer samples were fabricated by cutting out 1-inch diameter samples from thin film sheets using a bow punch and an arbor press or cutting 1-inch square samples with an Exacto knife. The samples were then marked with very small scribe marks to help distinguish the sample material and the side of the sample to be exposed to the space environment. Also, prior to flight, the samples dehydrated mass was obtained as discussed in reference 1. When the polymers were flown on the ISS, their corresponding control samples were stored on the ground at room temperature and pressure.

### *Photo Documentation*

After enduring space exposure and possible on-orbit contamination, the post-flight samples can display physical changes that include texturing, discoloration, tearing, or thickness erosion. A Sony Cyber-shot camera was used to document these changes by taking pictures of the same samples pre-flight and post-flight. In addition, the flight samples are photographed next to their corresponding control samples post-flight to display physical changes due to space exposure.

### *Optical Properties*

The number of layers scanned for optical properties was typically determined by the number of layers visibly effected by space exposure. Occasionally more than one layer was scanned. An equal number of layers of the flight sample and control sample were scanned to ensure an equivalent comparison.

A Cary 5000 spectrophotometer, operating with a DRA 2500 integrating sphere, was used to obtain spectral total and diffuse reflectance ($TR_\lambda$ and $DR_\lambda$, respectively) and spectral total and diffuse transmittance ($TT_\lambda$ and $DT_\lambda$, respectively) from 250 to 2,500 nm wavelengths. A baseline and zero scan is required prior to each optical property scan. For the baseline scan of $TR_\lambda$, a standard was placed in the integrating sphere sample holder. To scan for the zero scan, the standard was removed. For $TR_\lambda$, each sample was placed in the anterior sample holder and scanned. The $DR_\lambda$ zero and baseline scans are the same as $TR_\lambda$ except for the addition of a light absorbing trap positioned on the integrating sphere to receive the sample's spectrally reflected light. To obtain the zero scans for $TT_\lambda$, a small piece of opaque material was inserted in the spectrophotometer to block the beam of light from passing through. Then, the opaque material was removed and the flight or control sample was placed in the front of the sphere. The $DT_\lambda$ baseline and zero scans were the same except for removing the standard from the anterior sample holder during the sample scan so that specular light passing through the sample would be trapped in the light-tight chamber behind the sample.

A NASA Glenn Research Center Cary 5000 Excel Macro was used to compute the spectral specular reflectance ($SR_\lambda$) for 250 – 2500 nm from the difference between $TR_\lambda$ and $DR_\lambda$ ($SR_\lambda = TR_\lambda - DR_\lambda$). Likewise, the spectral specular transmittance ($ST_\lambda$) was computed for 250 – 2500 nm from the difference of $TT_\lambda$ and $DT_\lambda$ ($ST_\lambda = TT_\lambda - DT_\lambda$). The Excel Macro also computed the spectral absorptance ($\alpha_\lambda$), which was determined using the equation $\alpha_\lambda = 1 - (TR_\lambda + TT_\lambda)$. Finally, the Excel Macro was used to integrate each spectral curve into the air mass zero (AM0) solar spectrum (see Figure 8) over the spectral range (250 – 2500 nm) to get the following total AM0 integrated values: total reflectance (TR), diffuse reflectance (DR), specular reflectance (SR), total transmittance (TT), diffuse transmittance (DT), specular transmittance (ST) and solar absorptance ($\alpha_s$).

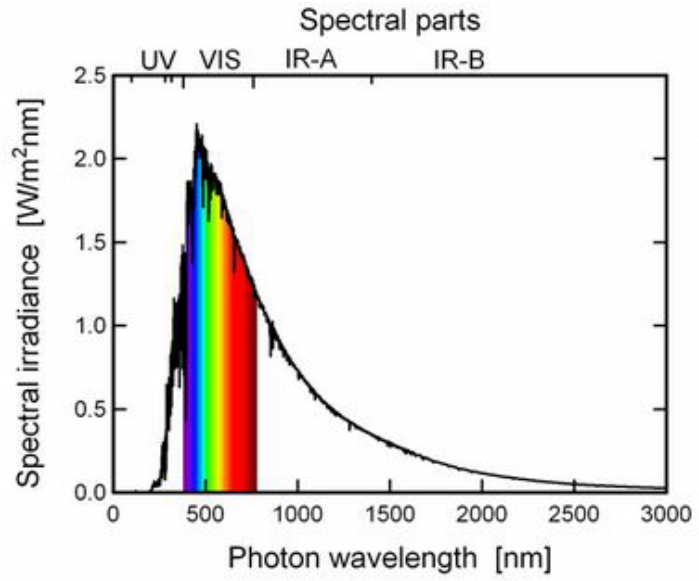


*Figure 8. Air mass zero (AM0) solar spectrum.*[11]

## Results and Discussion

### *MISSE 7B Ram Polymers Optical Properties*

The optical properties of only seven MISSE 7B ram flight samples with their corresponding controls were obtained because many of the samples were 0.75" x 0.75" (1.9 cm x 1.9 cm) square, which was determined to be too small for obtaining optical measurements. Attempts were made to scan the smaller samples using a Cary 5000 Small Spot Kit, but the spectral data was found to be too noisy and unreliable. Therefore, the 0.75" flight samples were not characterized for optical properties. In addition, the control samples were not available for comparison for four 1" samples, and one larger sample flown over a pinhole camera had a hole in the middle so it was not scanned either. Therefore, the samples which were not characterized for optical properties are not listed in this paper. The majority of the MISSE 7A zenith flight samples were analyzed for optical properties as their size (1" square) was large enough for measurements.

Table 4 lists the MISSE 7 ram samples along with their integrated optical properties. The remaining space exposed layer of each sample was scanned (note: all samples were 1 layer samples except B7-8 Kapton H in which 4 layers were flown). The graphs and photographs of the flight and control samples are provided in Figures 9-16. As can be seen in the data in Table 4 and the spectral data in Figure 15, the alumina contamination slide (E13) had very little change in the $\alpha_s$ (0.005) indicating very little on-orbit contamination occurred.

Table 4. Optical Property Data for MISSE 7 Ram Samples.

| MISSE ID | Material | Flight vs Control | TR | DR | SR | TT | DT | ST | $\alpha_s$ | $\Delta \alpha_s$ |
|---|---|---|---|---|---|---|---|---|---|---|
| B7-8 | Kapton H | Flight | 0.070 | 0.050 | 0.021 | 0.561 | 0.314 | 0.247 | 0.368 | 0.039 |
| | | Control | 0.112 | 0.007 | 0.105 | 0.559 | 0.012 | 0.547 | 0.329 | |
| B7-9 | Vespel | Flight | 0.166 | 0.163 | 0.003 | 0.179 | 0.179 | 0.000 | 0.655 | -0.001 |
| | | Control | 0.183 | 0.166 | 0.018 | 0.161 | 0.144 | 0.017 | 0.656 | |
| B7-1 | White Tedlar | Flight | 0.701 | 0.699 | 0.001 | 0.077 | 0.077 | 0.000 | 0.222 | -0.070 |
| | | Control | 0.622 | 0.619 | 0.004 | 0.086 | 0.085 | 0.000 | 0.292 | |
| B7-2 | White Tedlar with 0.5 mil Kapton H | Flight | 0.710 | 0.710 | 0.000 | 0.075 | 0.075 | 0.000 | 0.215 | -0.078 |
| | | Control | 0.621 | 0.617 | 0.005 | 0.086 | 0.085 | 0.001 | 0.293 | |
| B7-3 | White Tedlar with 1.0 mil Kapton H | Flight | 0.710 | 0.710 | 0.000 | 0.072 | 0.072 | 0.000 | 0.218 | -0.075 |
| | | Control | 0.622 | 0.618 | 0.004 | 0.085 | 0.084 | 0.001 | 0.293 | |
| E14 | Polypropylene (PP) | Flight | 0.191 | 0.185 | 0.006 | 0.684 | 0.664 | 0.020 | 0.125 | 0.050 |
| | | Control | 0.086 | 0.035 | 0.051 | 0.840 | 0.339 | 0.500 | 0.075 | |
| E13 | $Al_2O_3$ Contamination Slide | Flight | 0.141 | 0.003 | 0.137 | 0.856 | 0.003 | 0.853 | 0.003 | 0.005 |
| | | Control | 0.142 | 0.004 | 0.139 | 0.859 | 0.003 | 0.856 | -0.002 | |

Figure 9 provides a post-flight photograph of the B7-8 Kapton H flight and control samples and the corresponding absorptance spectra. As can be seen in the left side of Figure 9a, the top layer of the 4 layered B7-8 Kapton H flight sample was completely eroded away (except the edge which was protected by the sample holder). The second layer eroded such that a very fragile gossamer-thin layer peeled off from the top of the layer. This gossamer layer is seen as the curled up bright yellow layer on top of the underlying second layer in Figure 9a. Therefore, the gossamer layer was carefully removed and the remaining 2nd layer was scanned for optical properties. The flight sample $\alpha_s$ was 0.368, which was an increase of 0.039 as compared to the control sample due to the AO texturing.

Figure 10 provides a post-flight photograph of the single layer B7-9 Vespel flight and control samples and the corresponding $\alpha$ spectra. As can be seen in Figure 10a, the flight sample is a little brighter and matte as compared to the control sample. Although the $\alpha_s$ was essentially unchanged between the flight and control samples (0.655 and 0.656, respectively), the flight sample had increased absorptance spectral data in the short wavelengths (about 700 nm and below) and decreased absorptance spectral data in the longer wavelengths (in the IR, 700 nm and above). This can be seen in Figure 10b. This "cross-over" effect was seen in other spectra.

Figure 11 provides a post-flight photograph of the single layer B7-1 white Tedlar flight and control samples and the corresponding $\alpha$ spectra. This white Tedlar flight sample was flown without a thin Kapton cover and was exposed to an AO fluence of $4.22 \times 10^{21}$ atoms/cm$^2$. As seen in Figure 11a, the white Tedlar became brighter with space exposure. The $\alpha_s$ reflected this increase in brightness with the flight sample having a lower $\alpha_s$ (0.222) than the control sample (0.292). Hence, the $\alpha_s$ of flight sample decreased 0.070 (24%) compared to the control sample. The increase in brightness is due to the buildup of AO durable white $TiO_2$ particles on the surface. MISSE experiment erosion data has shown that the $E_y$ of white Tedlar decreases with increasing AO fluence.[1,12] The decreased $E_y$ with increased AO fluence for white Tedlar is also attributed to a buildup of AO durable $TiO_2$ particles on the surface of the sample with increasing AO exposure. The $TiO_2$ protects the underlying material from erosion if undisturbed, thus decreasing the $E_y$ with increasing AO fluence; and since $TiO_2$ is an effective sunscreen material it is also expected to increase UV durability.

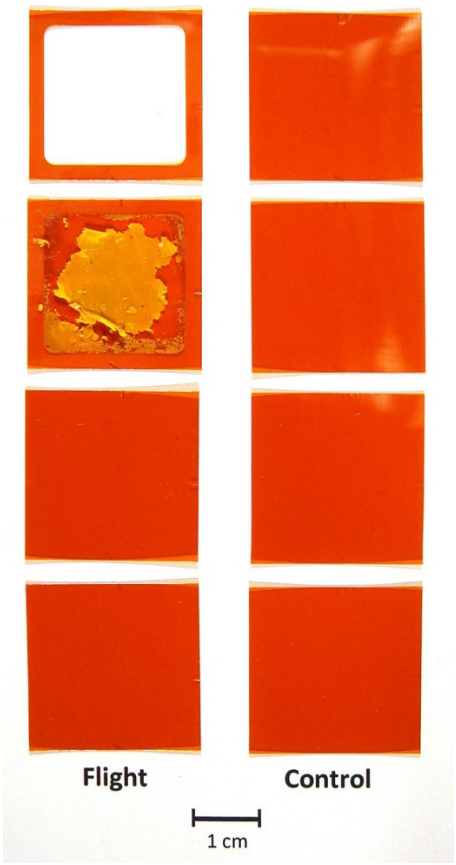


a.

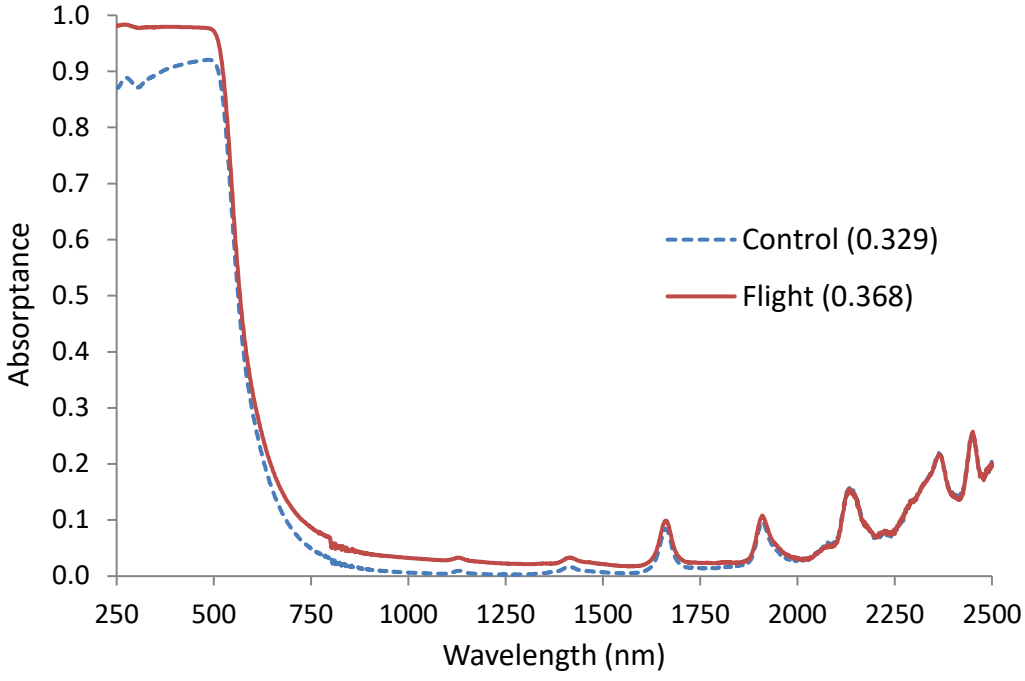


b.

*Figure 9. MISSE 7B ram B7-8 Kapton H: a). Post-flight photograph of the flight and control samples, top layers are at the top of the image and b). Absorptance curves for the flight (0.368) and control (0.329) samples.*

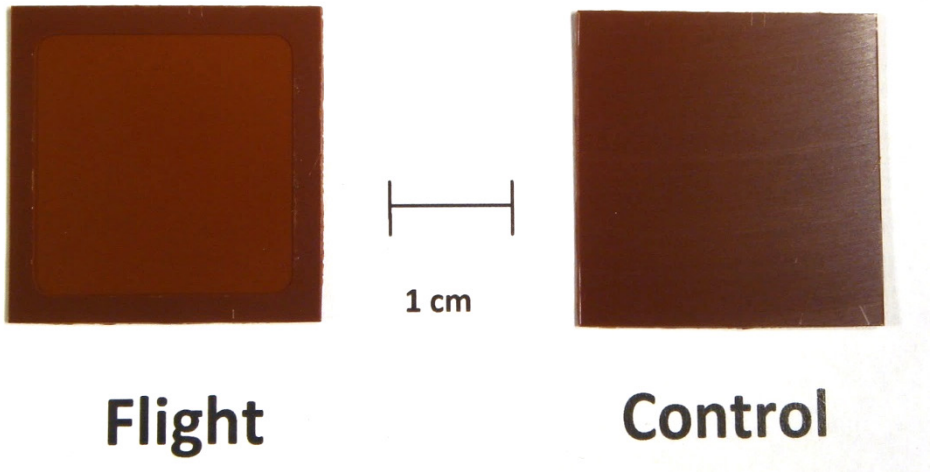


a.

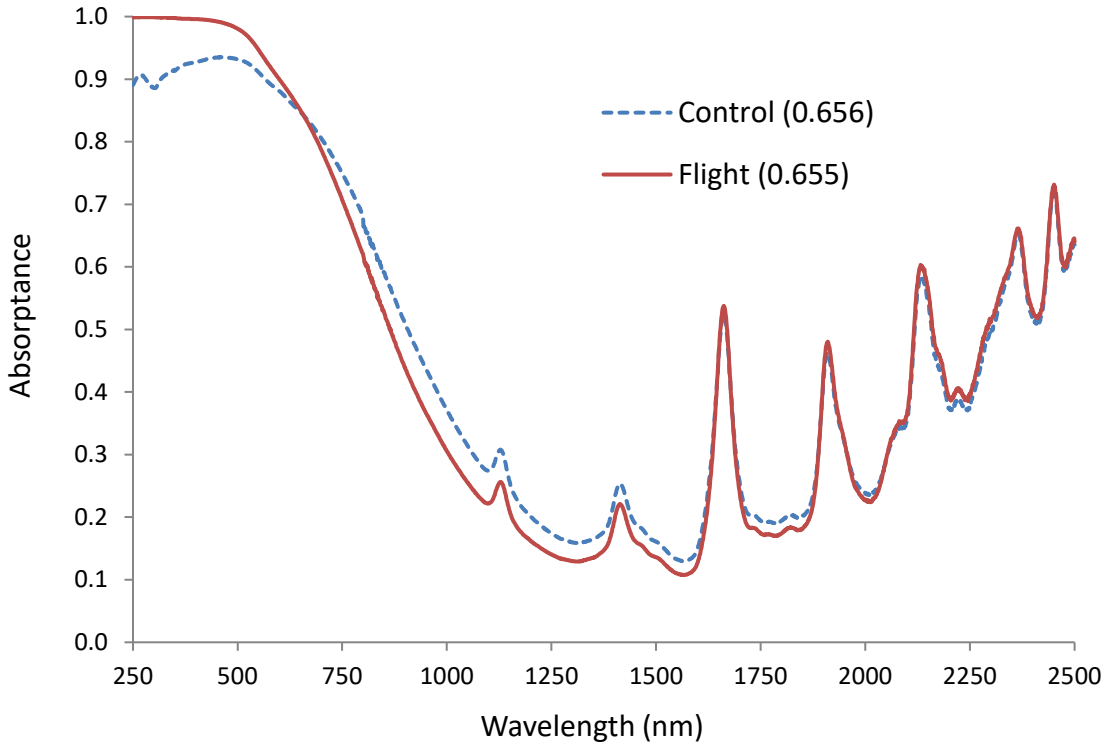


b.

*Figure 10. MISSE 7B ram B7-9 Vespel: a). Post-flight photograph of the flight and control samples, and b). Absorptance curves for the flight (0.655) and control (0.656) samples.*

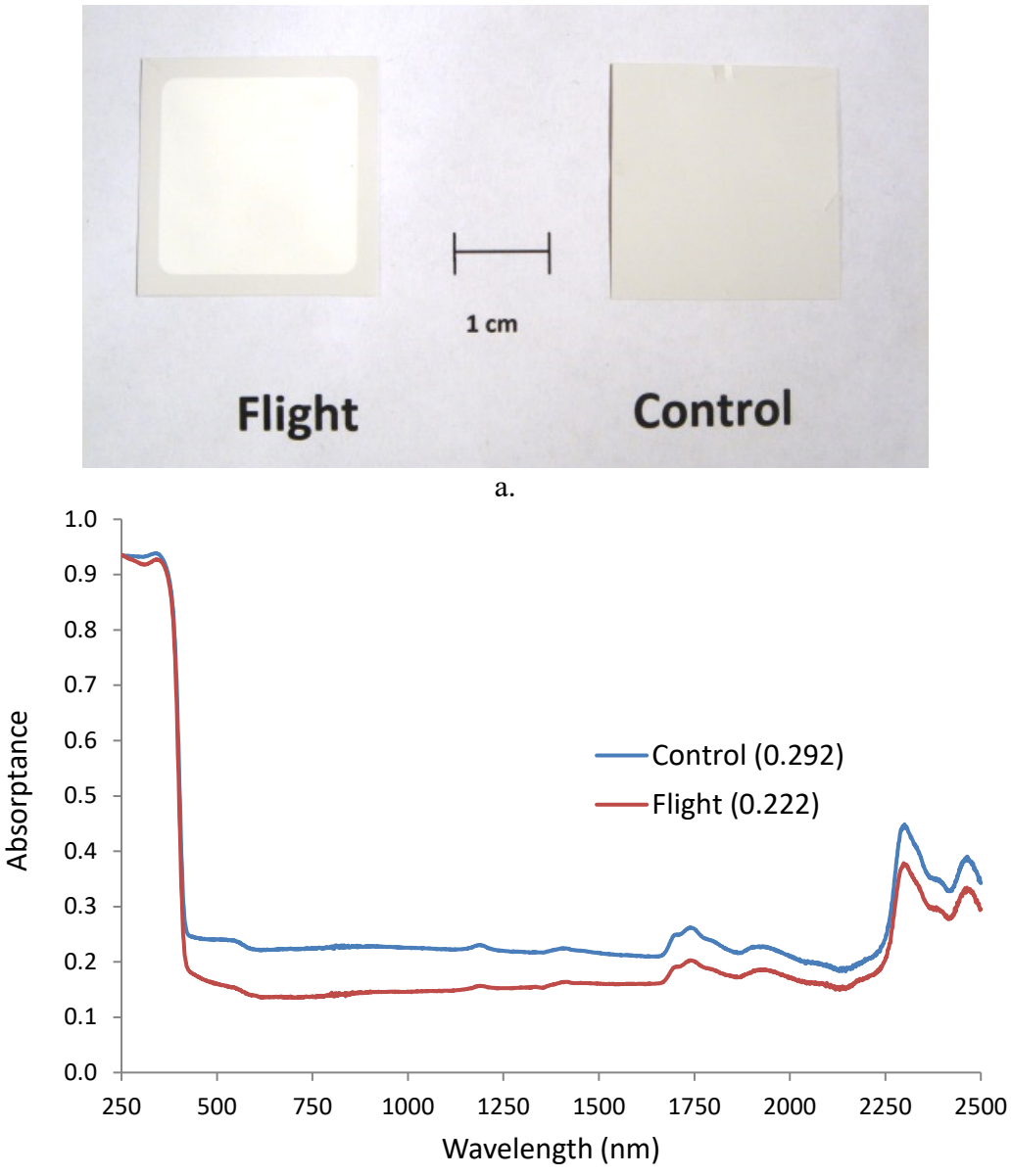


*Figure 11. MISSE 7B ram B7-1 white Tedlar PVF: a). Post-flight photograph of the flight and control samples, and b). Absorptance curves for the flight (0.222) and control (0.292) samples.*

Figure 12 provides a post-flight photograph of the B7-2 white Tedlar flight and control samples and the corresponding α spectra. In Figure 12a, the 0.5 mil Kapton H cover for the flight sample is included in the photograph, but the 0.5 mil Kapton cover for the control sample is not included. As can be seen in Figure 12a, the flight sample 0.5 mil Kapton cover was completely eroded away except for the edge, which was protected from AO exposure by the flight holder. Thus, the B7-2 white Tedlar sample was exposed to an AO fluence of 3.79 x $10^{21}$ atoms/cm$^2$. Similar to B7-1, B7-2 white Tedlar became brighter with space exposure. The $\alpha_s$ of B7-2 flight sample decreased 0.078 (26.6%) compared to the control sample.

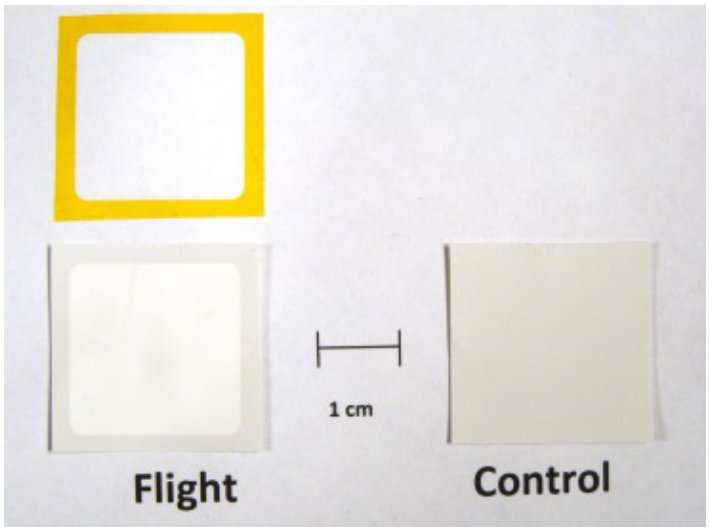


a.

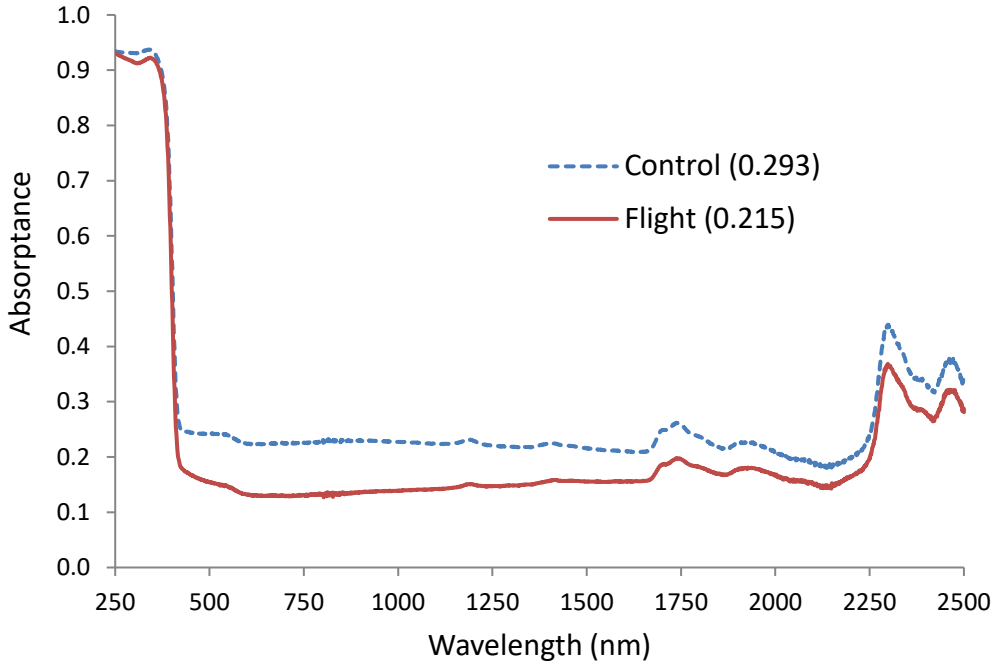


b.

*Figure 12. MISSE 7B ram B7-2 white Tedlar (flown with a 0.5 mil Kapton cover): a). Post-flight photograph of the flight and control samples, and b). Absorptance curves for the flight (0.215) and control (0.293) samples.*

It is important to note that even though the white Tedlar sample appears visually to be opaque, non-visible light wavelengths were found to transmit through the sample in the infrared (IR) region. Figure 13 (a-f) provides the six data graphs (total, diffuse, and specular reflectance and total, diffuse, and specular transmittance) for the B7-2 0.5 mil Kapton H covered white Tedlar sample with Kapton H removed. The diffuse and total transmittance in the IR region can be seen in Figures 13b and 13f, respectively.

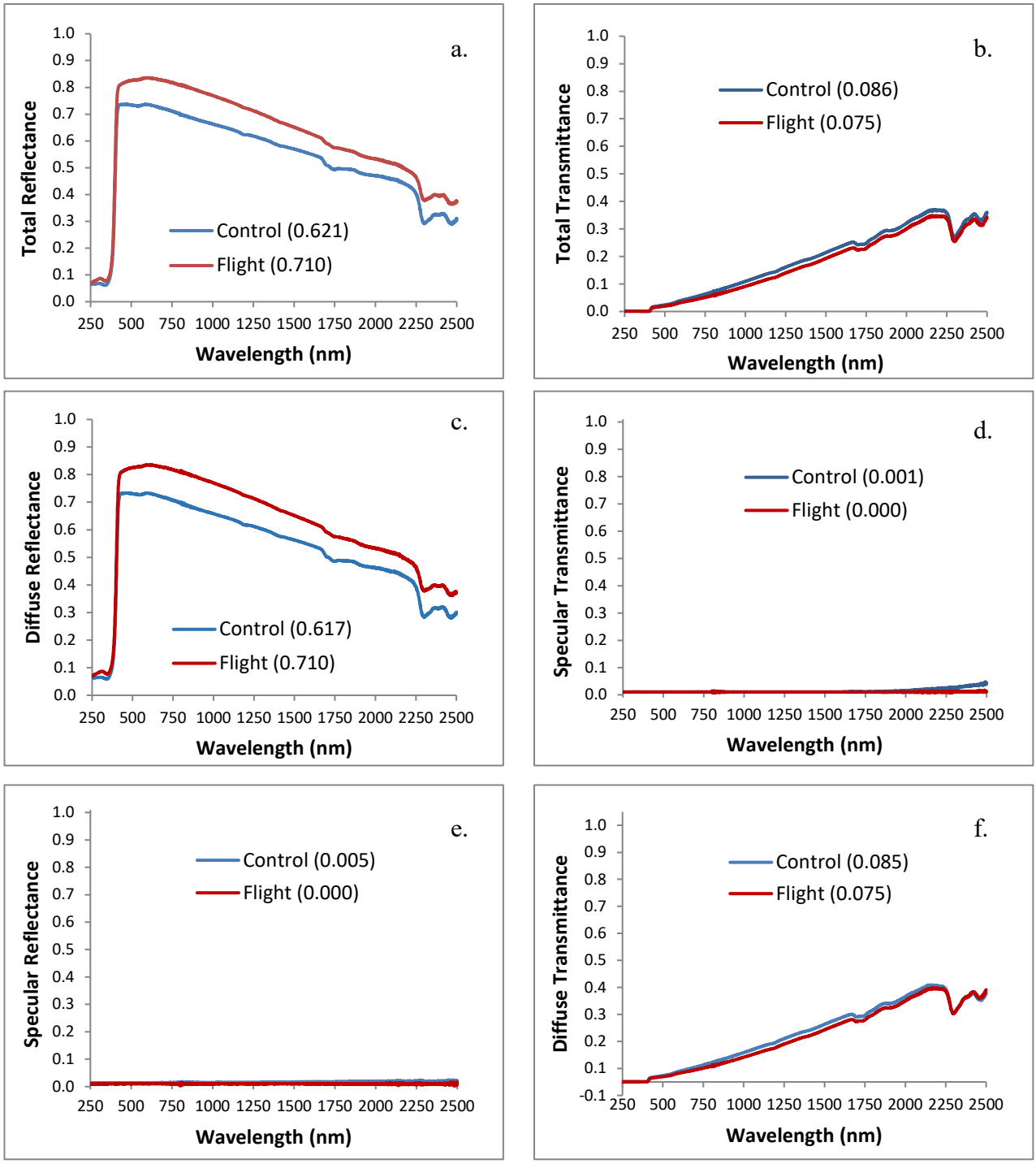


*Figure 13. The optical property graphs of white Tedlar (B7-2) showing increases in reflectance and small decrease in transmittance of the flight samples as compared to the control. (a) TR, (b) TT, (c) DR, (d) ST, (e) SR, and (f) DT.*

Figure 14 provides a post-flight photograph of the B7-3 white Tedlar flight and control samples and the corresponding $\alpha$ spectra. In Figure 14a, the 1.0 mil Kapton H cover for the control sample is not included in the photograph. Like the B7-2 sample, the 1.0 mil Kapton cover for the B7-3 flight sample was completely eroded away except at the protected edge. Thus, the B7-3 white Tedlar sample was exposed to an AO fluence of 3.37 x $10^{21}$ atoms/cm$^2$. Although the B7-2 and B7-3 samples experienced a lower AO fluence than the B7-1 sample, the white Tedlar became bright like the B7-1 sample. Even though B7-1, B7-2, and B7-3 experienced different amounts of AO exposure due to the use of different thicknesses of Kapton H covers, the changes in $\alpha_s$ (-0.070, -0.078, -0.075, respectively) are close which indicates the brightness of white Tedlar stabilizes with AO exposures of 3.37 x $10^{21}$ atoms/cm$^2$ and above.

Figure 15 provides a post-flight photograph of the E14 Polypropylene (PP) flight and control samples and the corresponding $\alpha$ spectra. As can be seen in Figure 15a, the flight sample has become darker, slightly yellowed and it is also very matte. Due to the coloring of the flight sample from space exposure the total reflectance of the sample increased from 0.086 to 0.191 with a large increase in diffuse reflectance from 0.035 to 0.185, as compared to the control sample. The specular reflectance of the flight sample decreased from 0.051 to 0.006 due to the sample becoming very matte. The total and specular transmittance of PP became lower after space exposure, due to slight darkening and texturing of the previously clear sample, from 0.840 to 0.684 and from 0.500 to 0.020, respectively. And, the diffuse transmittance of the sample increased from 0.339 to 0.664 due to the matte texture. Overall, the space exposure caused a 0.05 increase (67%) in $\alpha_s$ of the PP sample, an increase from 0.075 to 0.125.

The aluminum oxide slide, or alumina slide (E13) was flown to determine the level of contamination the flight samples received on-orbit. Figure 16 provides a post-flight photograph of the alumina flight and control samples and the corresponding $\alpha$ spectra. As can be seen in Figure 16a, there is no visible difference between the flight and control samples. This is consistent with the optical properties listed in Table 4, and in the absorptance spectra provided in Figure 16b. As seen in the $\alpha$ spectra, there is a very small increase in absorptance in the UV region, but the $\alpha_s$ of the flight sample was very low (0.003).

The PP sample (E14) and the white Tedlar samples (B7-1, B7-2, B7-3) provide a comparison of polymers that respond differently in the space environment. The PP flight sample became darker and had the greatest increase in $\alpha_s$ of 0.050, with corresponding increases in DR, DT, TR, and TT. On the other hand, all three white Tedlar flight samples were brighter than the controls, and the corresponding $\alpha$ curve is lower than the control sample $\alpha$ curve (i.e., lower solar absorptance). The white Tedlar with a 0.5 mil Kapton H sacrificial cover has the greatest decrease in $\alpha_s$ with a value change of -0.078 (a 27% decrease). When comparing the three white Tedlar samples, the change in brightness was found to have stabilized with the lowest AO fluence of 3.37 x $10^{21}$ atoms/cm$^2$, and higher fluence exposures did not significantly change white Tedlar's color or optical properties (including $\alpha_s$) further.

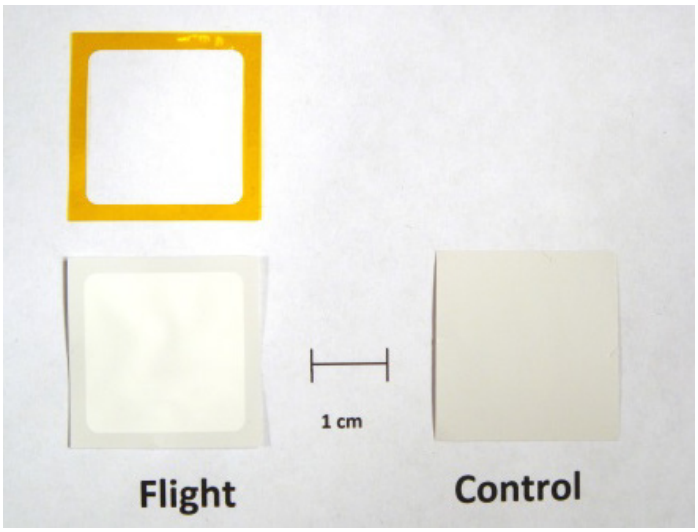


a.

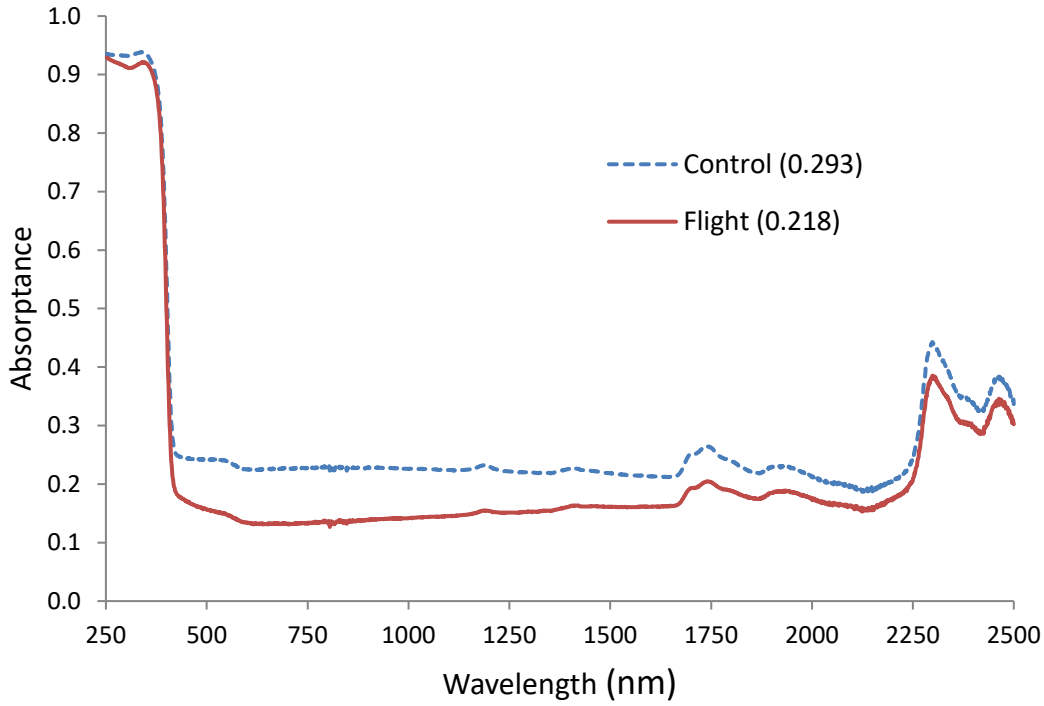


b.

*Figure 14. MISSE 7B ram B7-3 white Tedlar (flown with a 1 mil Kapton cover): a). Post-flight photograph of the flight and control samples, and b). Absorptance curves for the flight (0.218) and control (0.293) samples.*

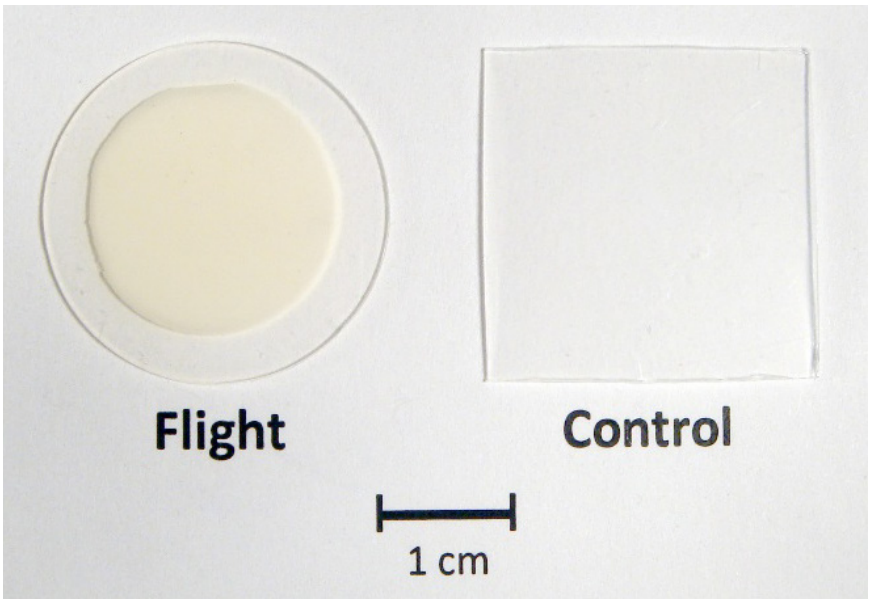


a.

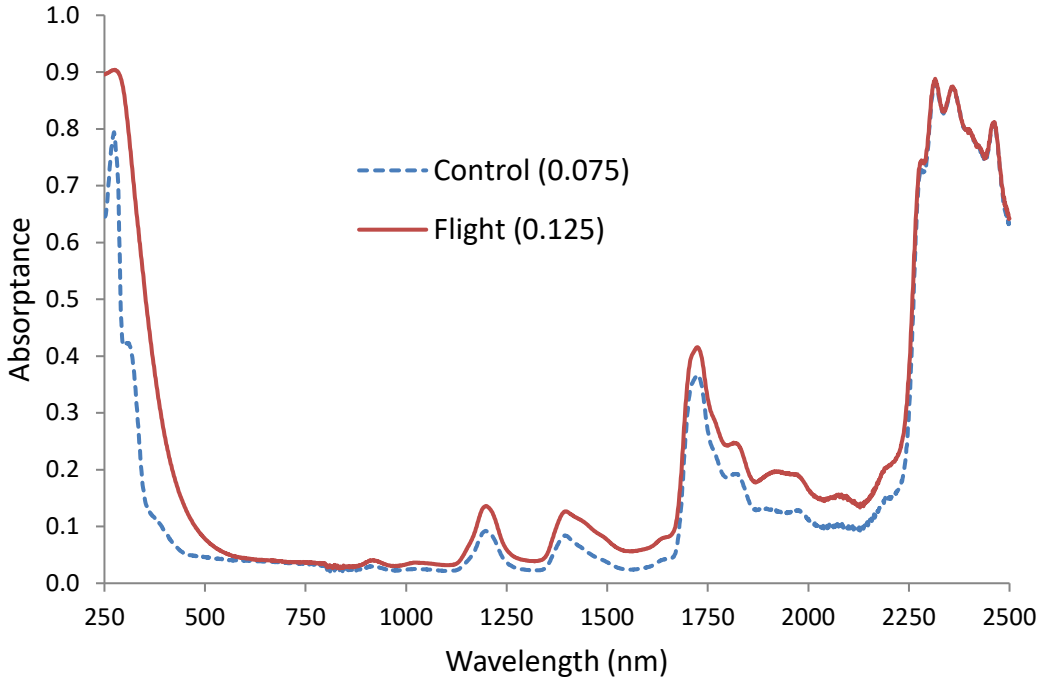


b.

*Figure 15. MISSE 7B ram E14 Polypropylene: a). Post-flight photograph of the flight and control samples, and b). Absorptance curves for the flight (0.125) and control (0.075) samples.*

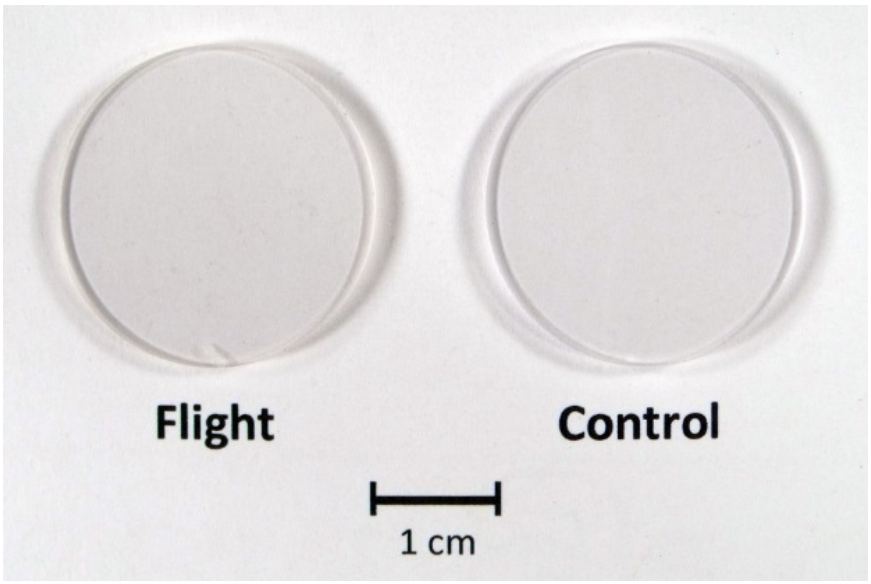


a.

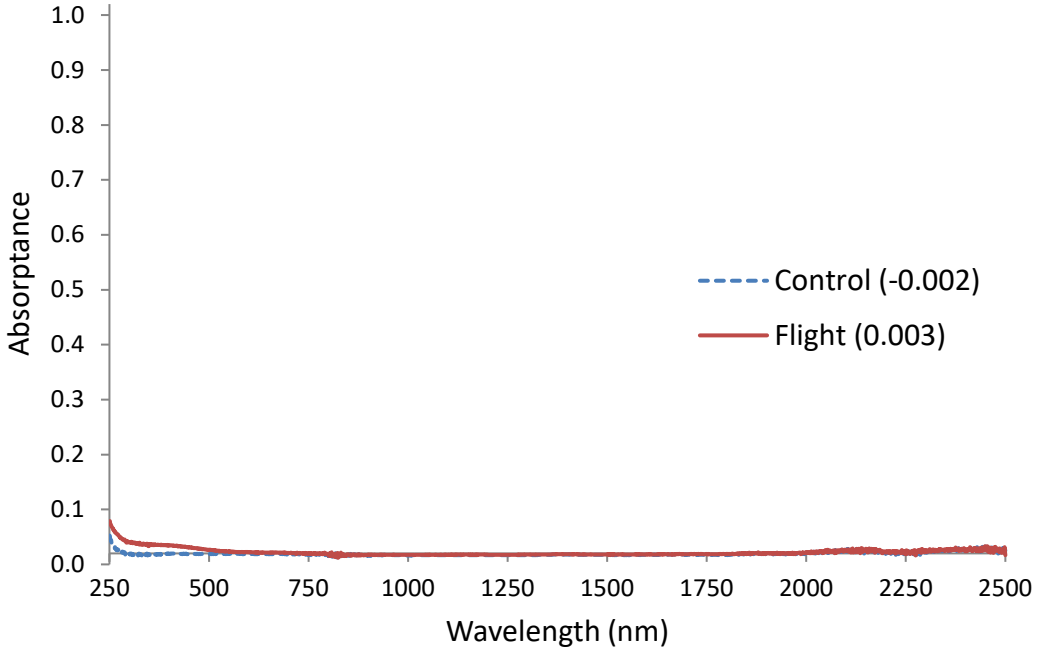


b.

*Figure 16. MISSE 7B ram E13 $Al_2O_3$ Contamination Slide: a). Post-flight photograph of the flight and control samples, and b). Absorptance curves for the flight (0.003) and control (-0.002) samples.*

### *MISSE 7A Zenith Polymers Optical Properties*

Table 5 lists the MISSE 7 zenith samples along with their integrated optical properties. The 4th column lists the number of layers scanned (#LS) over the number of layers flown (#LF). The graphs and post-flight photographs of the flight and control samples are provided in Figures 17-31. It should be noted that the optical data for PVDF (Z-5) and ECTFE (Z-6) has been up-dated since the data was originally presented.[14]

Three materials were not significantly affected by the space exposure: PTFE (Z-1), FEP (Z-2) and Si/Kapton E/Al (Z-12). As shown in Figure 17 the 1 layer PTFE flight sample looks similar to the control sample (Figure 17a) and the PTFE flight sample experienced a solar absorptance increase that was limited to UV wavelengths under 400 nm (Figure 17b). The overall absorptance change between the control and flight samples was negligible ($\Delta\ \alpha_s = 0.001$). Figure 18 shows that the response of uncoated FEP to LEO exposure was similar to PTFE's, with no visible change (Figure 18a) and increases in absorptance limited to the lower UV wavelengths with a small $\Delta\alpha_s$ of 0.001 (Figure 18b). Figure 28 shows that the absorptance of Si/Kapton E/Al was similarly not affected by the space exposure, with a -0.002 $\alpha_s$ change being within experimental error. The reflectance of the slightly curved flight and control samples in Figure 28a provides an appearance of a visual change, but this is just due to reflected light. No visible change was observed.

Figure 19 shows that the LEO zenith exposure increased the solar absorptance of CTFE (Z-3) substantially in the UV wavelengths, resulting in a doubling of $\alpha_s$ (0.021 to 0.042). Note that there was very little color change in the CTFE as compared to ETFE (Z-4) shown in Figure 20 and several others (PVDF (Z-5), ECTFE (Z-6) and PVF (Z-7)) which all experienced significant discoloration due to the LEO exposure. In Figure 20, the scan of the blue control ETFE sample drops slightly below zero between 600-750 nm. This is within error for the instrument. Space exposure darkened ETFE, as shown in Figure 20a, and increased the absorptance significantly from 0.015 to 0.087 with increases most noticeable in the wavelengths from approximately 800 nm and below, as shown in Figure 20b. The level of browning in ETFE was moderate compared to PVDF (Z-5), ECTFE (Z-6) and PVF (Z-7); these higher levels of browning were accompanied by further increases in absorptance.

As shown in Figure 21a the top layer of the 2 layered PVDF (Z-5) sample darkened significantly, and the 2nd (underlying later) was also darkened. Figure 21b provides $\alpha_s$ curves for the top space exposed layer (1 layer scan), whereas Figure 21c provides $\alpha_s$ curves for both layers scanned together (2 layer scan). For the single layer scan, the absorptance increased from the control sample of 0.045 to 0.151. For the two layer scan, the absorptance increased from 0.040 to 0.173.

High levels of browning were observed in ECTFE (Z-6), shown in Figure 22a. Figure 22b provides $\alpha_s$ curves for the top space exposed layer (1 layer scan), whereas Figure 22c provides $\alpha_s$ curves for all three layers scanned together (3 layer scan). For the single layer scan, the absorptance increased from the control sample of 0.011 to 0.250. For the three layer scan, the absorptance increased from 0.036 to 0.261. Both the single and 3 layer ECTFE spectra (Figures 22b and 22c, respectively) shows an odd jump in the flight data at 800 nm; this is an artifact believed to be caused by the detector change in the equipment. The equipment was re-calibrated and the sample re-scanned several time, all of which had the jump.

Table 5. Optical Property Data for MISSE 7 Zenith Polymers.

| MISSE ID | Material | Flight vs Control | #LS/ #LF | TR | DR | SR | TT | DT | ST | $\alpha_s$ | $\Delta \alpha_s$ |
|---|---|---|---|---|---|---|---|---|---|---|---|
| Z-1 | PTFE | Flight | 1/1 | 0.135 | 0.124 | 0.011 | 0.808 | 0.339 | 0.469 | 0.057 | 0.001 |
| | | Control | | 0.144 | 0.134 | 0.010 | 0.800 | 0.340 | 0.460 | 0.056 | |
| Z-2 | FEP | Flight | 1/1 | 0.049 | 0.029 | 0.020 | 0.939 | 0.028 | 0.911 | 0.011 | 0.001 |
| | | Control | | 0.051 | 0.019 | 0.032 | 0.939 | 0.030 | 0.909 | 0.010 | |
| Z-3 | CTFE | Flight | 2/2 | 0.113 | 0.047 | 0.066 | 0.844 | 0.020 | 0.824 | 0.042 | 0.021 |
| | | Control | | 0.118 | 0.012 | 0.106 | 0.861 | 0.018 | 0.843 | 0.021 | |
| Z-4 | ETFE | Flight | 2/2 | 0.104 | 0.069 | 0.035 | 0.809 | 0.333 | 0.475 | 0.087 | 0.072 |
| | | Control | | 0.107 | 0.013 | 0.093 | 0.878 | 0.022 | 0.856 | 0.015 | |
| Z-5 | PVDF | Flight | 1/2 | 0.070 | 0.058 | 0.012 | 0.779 | 0.459 | 0.291 | 0.151 | 0.106 |
| | | Control | | 0.072 | 0.042 | 0.029 | 0.883 | 0.519 | 0.364 | 0.045 | |
| | | Flight | 2/2 | 0.113 | 0.106 | 0.008 | 0.713 | 0.563 | 0.151 | 0.173 | 0.133 |
| | | Control | | 0.132 | 0.094 | 0.038 | 0.828 | 0.644 | 0.184 | 0.040 | |
| Z-6 | ECTFE | Flight | 1/3 | 0.111 | 0.088 | 0.023 | 0.639 | 0.490 | 0.149 | 0.250 | 0.239 |
| | | Control | | 0.070 | 0.025 | 0.045 | 0.919 | 0.066 | 0.853 | 0.011 | |
| | | Flight | 3/3 | 0.191 | 0.150 | 0.041 | 0.549 | 0.415 | 0.133 | 0.261 | 0.225 |
| | | Control | | 0.177 | 0.066 | 0.111 | 0.788 | 0.148 | 0.64 | 0.036 | |
| Z-7 | PVF | Flight | 12/12 | 0.366 | 0.343 | 0.24 | 0.392 | 0.342 | 0.051 | 0.242 | 0.164 |
| | | Control | | 0.453 | 0.327 | 0.127 | 0.468 | 0.342 | 0.127 | 0.078 | |
| Z-8 | PI (Kapton H) | Flight | 3/3 | 0.182 | 0.126 | 0.056 | 0.351 | 0.174 | 0.177 | 0.467 | 0.029 |
| | | Control | | 0.201 | 0.03 | 0.17 | 0.361 | 0.028 | 0.333 | 0.438 | |
| Z-9 | Al-FEP* | Flight | 1/1 | 0.783 | - | - | 0 | 0 | 0 | 0.217 | 0.061 |
| | | Control | | 0.844 | - | - | 0 | 0 | 0 | 0.156 | |
| Z-10 | Ag-FEP* | Flight | 1/1 | 0.867 | - | - | 0 | 0 | 0 | 0.133 | 0.052 |
| | | Control | | 0.919 | - | - | 0 | 0 | 0 | 0.081 | |
| Z-11 | PE | Flight | 8/8 | 0.356 | 0.324 | 0.032 | 0.556 | 0.337 | 0.219 | 0.088 | 0.017 |
| | | Control | | 0.399 | 0.284 | 0.115 | 0.53 | 0.324 | 0.207 | 0.071 | |
| Z-12 | Si/Kapton E/Al | Flight | 1/1 | 0.579 | 0.037 | 0.542 | 0 | 0 | 0 | 0.421 | -0.002 |
| | | Control | | 0.576 | 0.042 | 0.535 | 0 | 0 | 0 | 0.423 | |
| Z-14 | $Al_2O_3$/FEP | Flight | 1/1 | 0.117 | 0.092 | 0.026 | 0.817 | 0.022 | 0.795 | 0.066 | 0.025 |
| | | Control | | 0.132 | 0.045 | 0.087 | 0.826 | 0.027 | 0.799 | 0.041 | |
| E9 | PP | Flight | 1/1 | 0.083 | 0.048 | 0.035 | 0.796 | 0.350 | 0.446 | 0.121 | 0.050 |
| | | Control | | 0.086 | 0.042 | 0.045 | 0.842 | 0.356 | 0.486 | 0.071 | |
| P13-Z | PVOH | Flight | 6/12 | 0.414 | 0.403 | 0.010 | 0.383 | 0.374 | 0.009 | 0.203 | 0.124 |
| | | Control | | 0.377 | 0.303 | 0.074 | 0.544 | 0.509 | 0.035 | 0.079 | |

#LS/#LF: # layers scanned/# layers flown
*FEP was space-facing

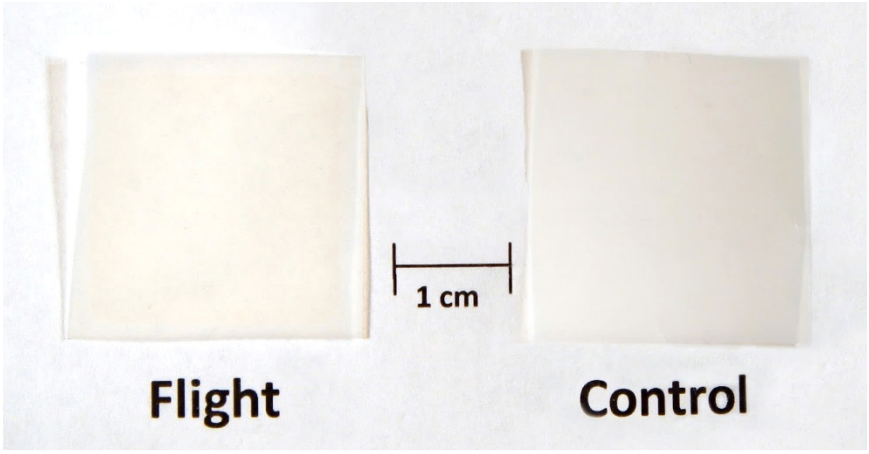


a.

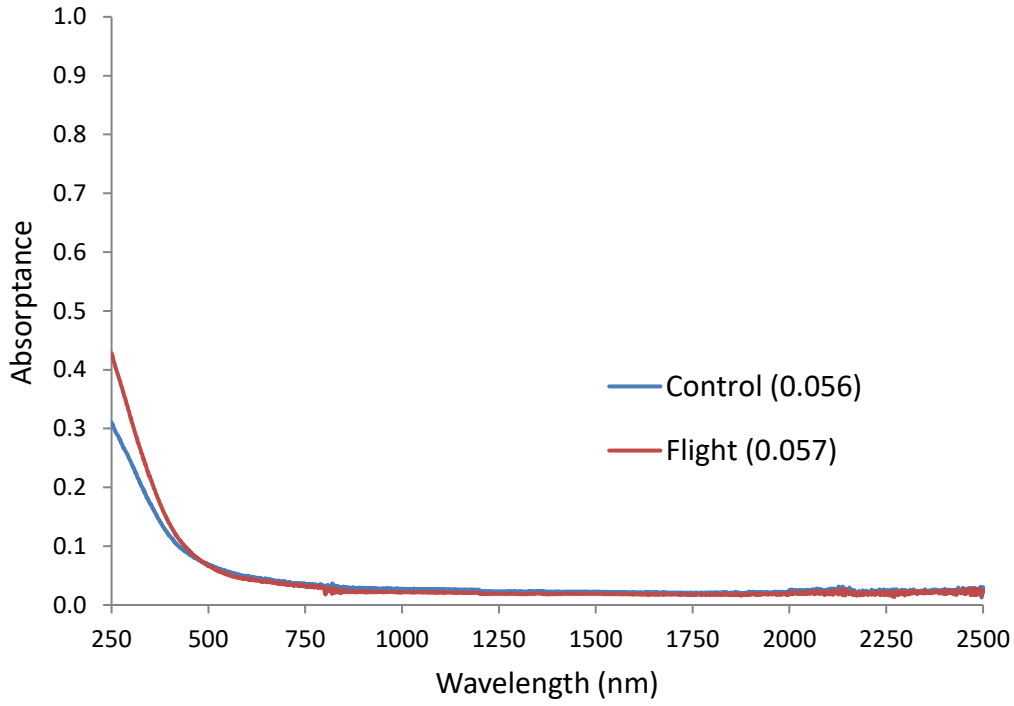


b.

*Figure 17. MISSE 7 Zenith Z-1 PTFE: a). Post-flight photograph of the flight and control samples, and b). Absorptance curves for the flight (0.057) and control (0.056) samples (1 layer).*

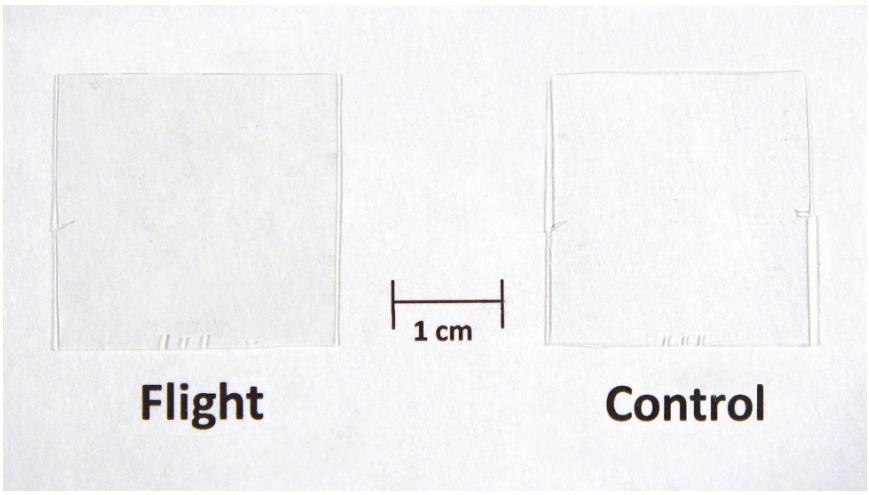


a.

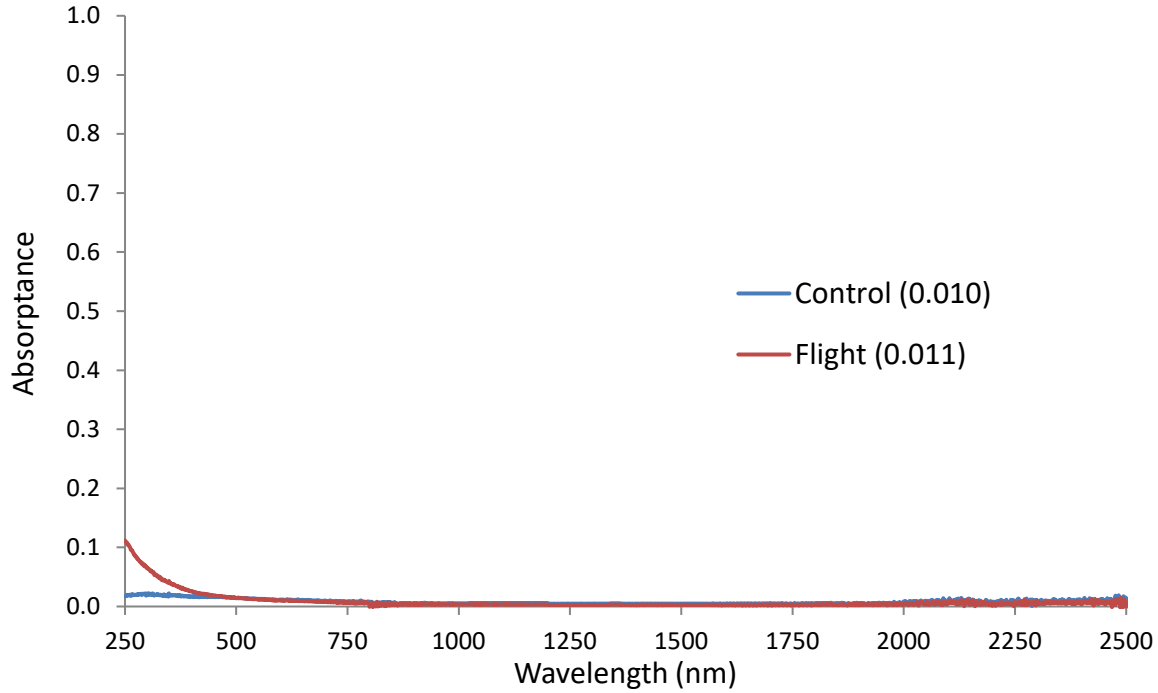


b.

*Figure 18. MISSE 7 Zenith Z-2 Teflon FEP: a). Post-flight photograph of the flight and control sample, and b). Absorptance curves for the flight (0.011) and control (0.010) samples (1 layer).*

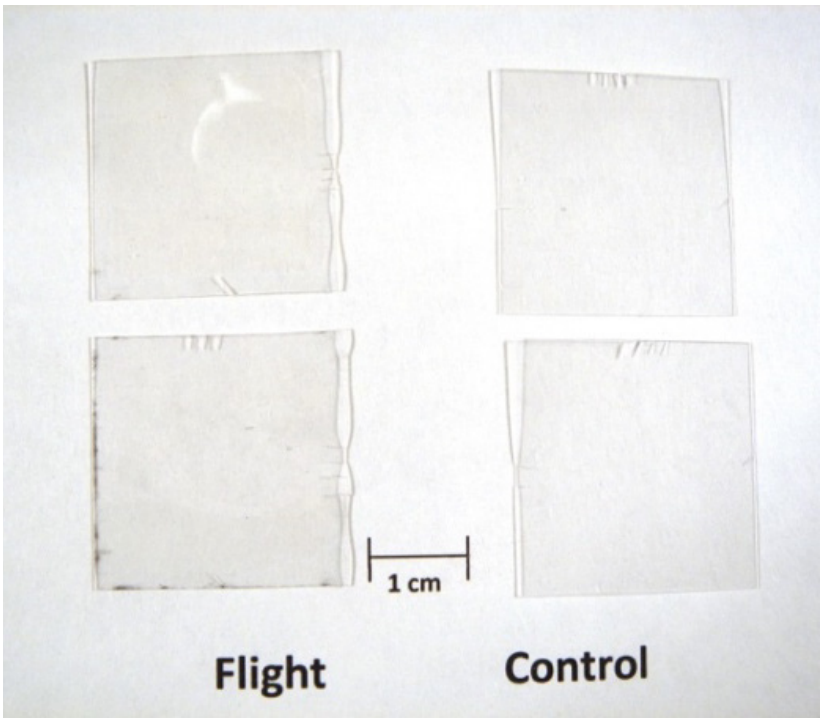


a.

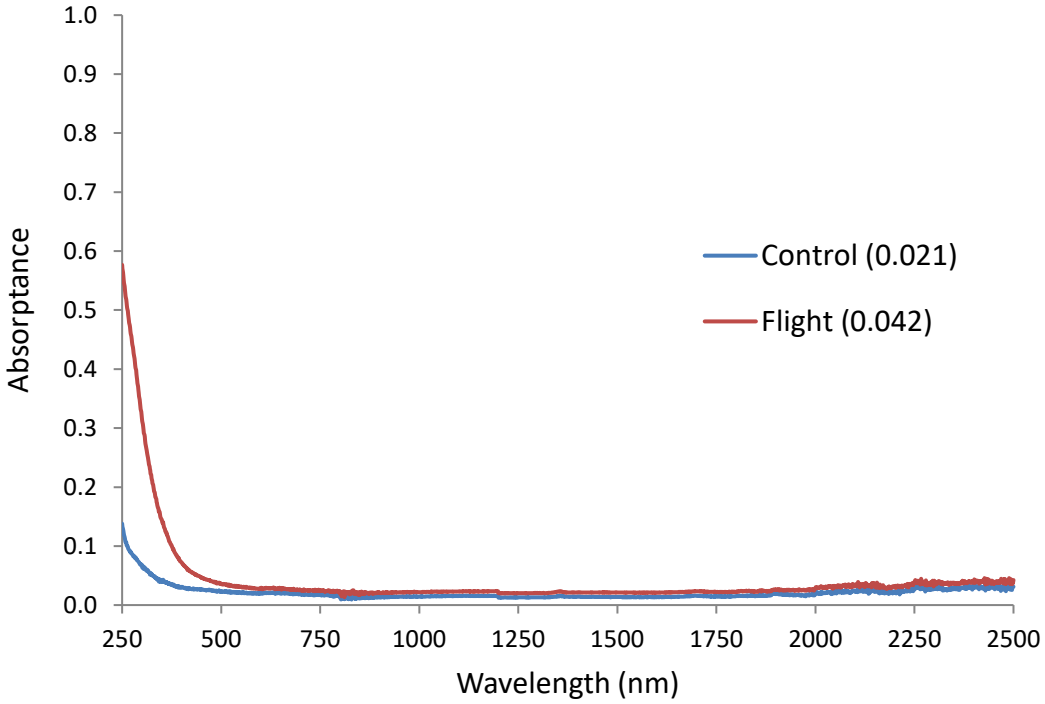


b.

*Figure 19. MISSE 7 Zenith Z-3 CTFE: a). Post-flight photograph of the flight and control sample, and b). Absorptance curves for the flight (0.042) and control (0.021) samples (2 of 2 layers).*

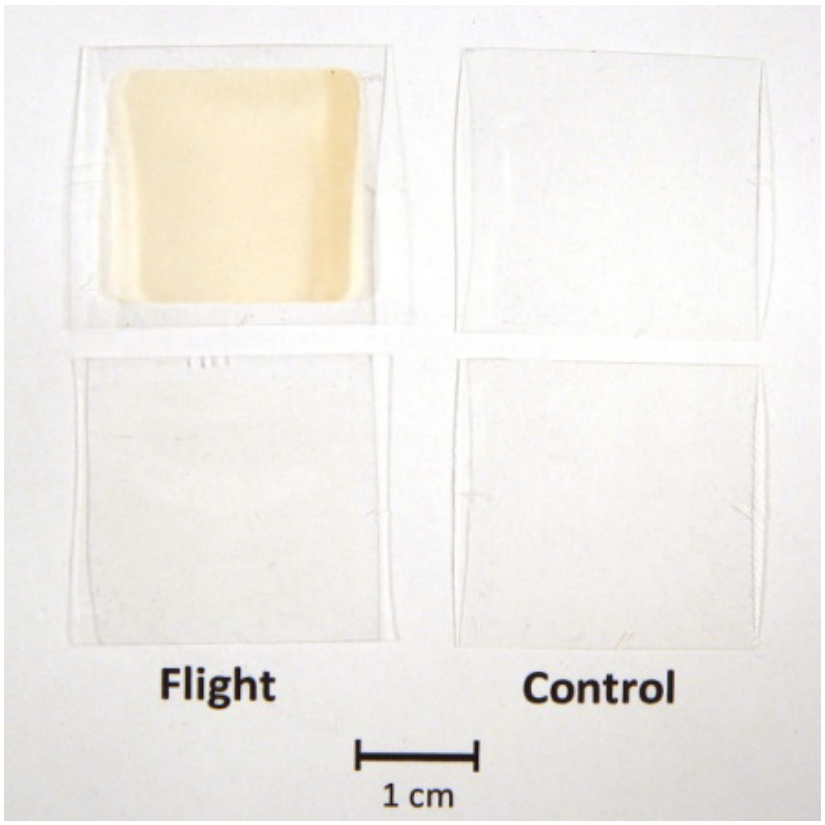


a.

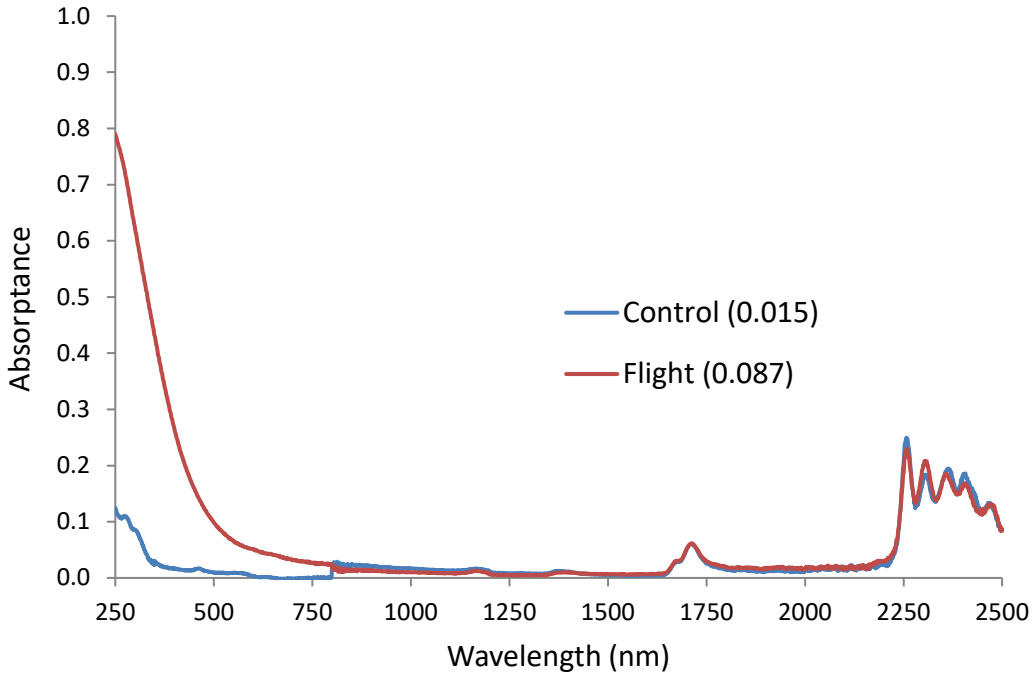


b.

*Figure 20. MISSE 7 Zenith Z-4 ETFE: a). Post-flight photograph of the flight and control sample, and b). Absorptance curves for the flight (0.087) and control (0.015) samples (2 of 2 layers).*

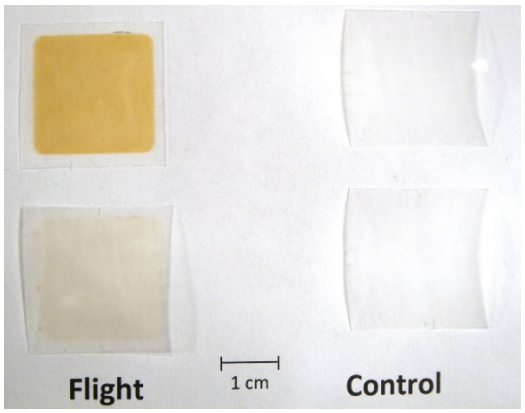


a.

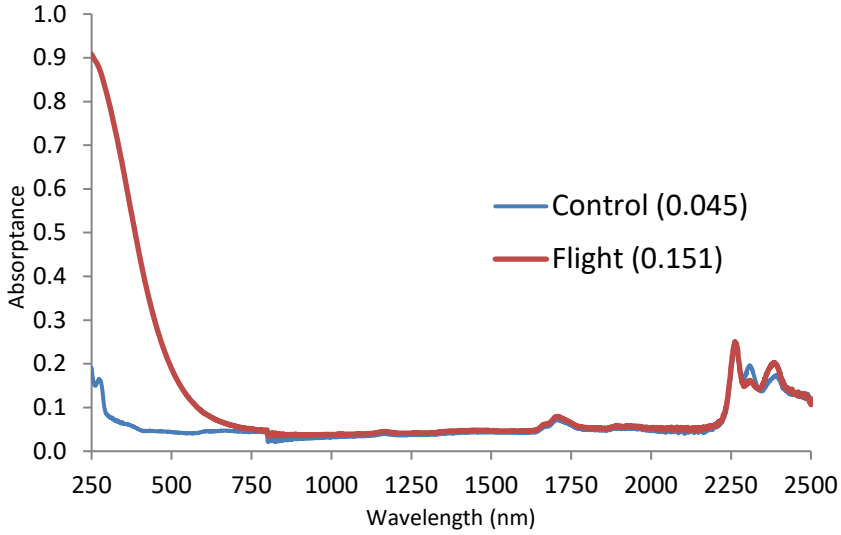


b.

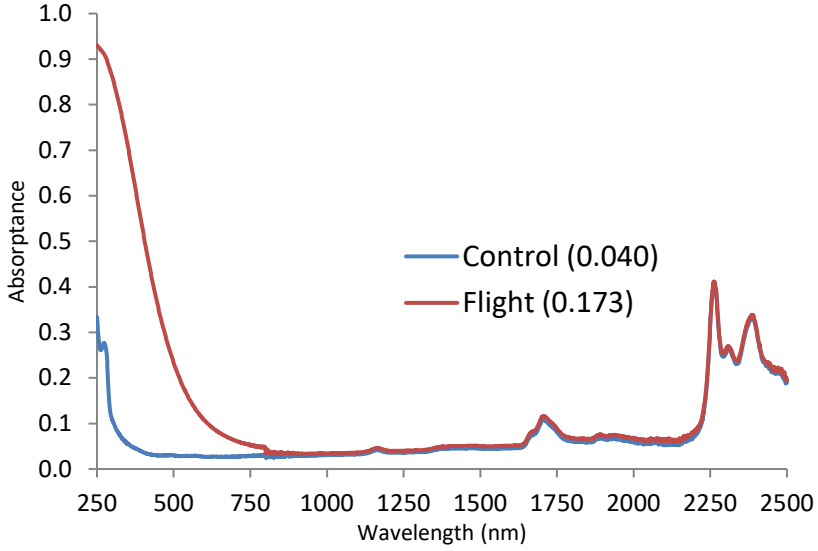


c.

*Figure 21. MISSE 7 Zenith Z-5 PVDF: a). Post-flight photograph of the flight and control samples, b). Absorptance curves for 1 layer of flight (0.171) and control (0.045) samples, and c). Absorptance curves for 2 layers of flight (0.173) and control (0.040) samples.*

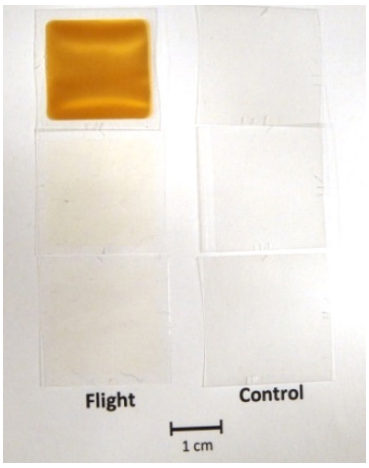


a.

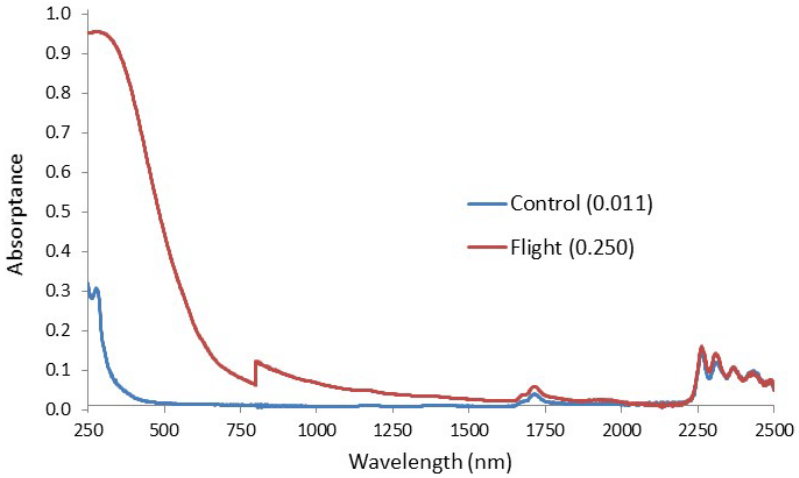


b.

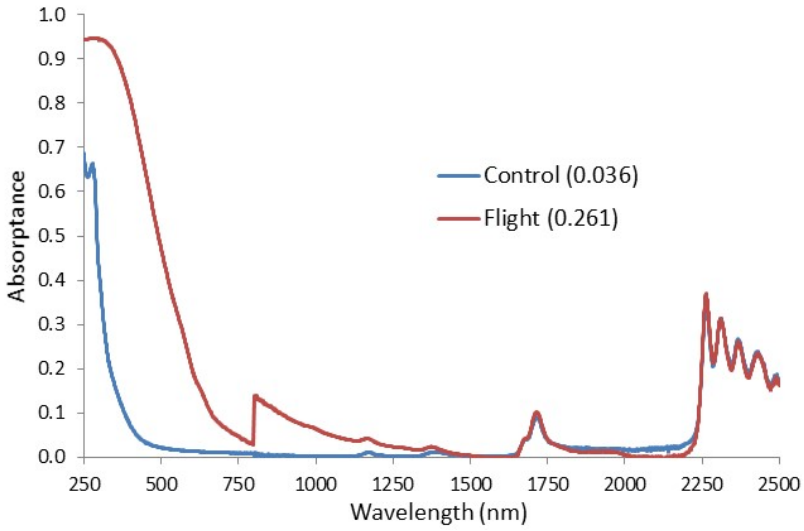


c.

*Figure 22. MISSE 7 Zenith Z-6 ECTFE: a). Post-flight photograph of the flight and control samples, b). Absorptance curves for 1 layer of flight (0.250) and control (0.011) samples, and c). Absorptance curves for 3 layers of flight (0.261) and control (0.036) samples.*

Figure 23a shows significant browning of the 12 layered PVF sample. The top space exposed layer is separated from the underlying 11 layers in Figure 23a. In this image, the stacked 11 layers of both the control and flight samples look darker than the single separated top layer. As shown in Figure 23b, the $\alpha_s$ increased from 0.078 for the 12 layered control sample to 0.242 for the 12 layered flight sample. The absorptance increases were limited to wavelengths below about 1100 nm.

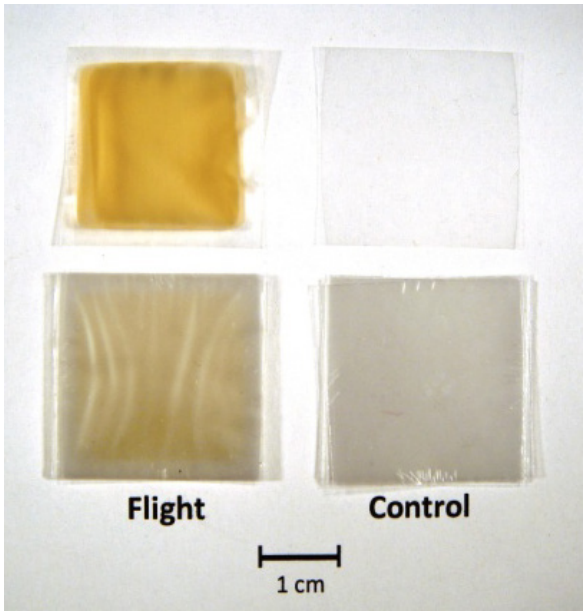


a.

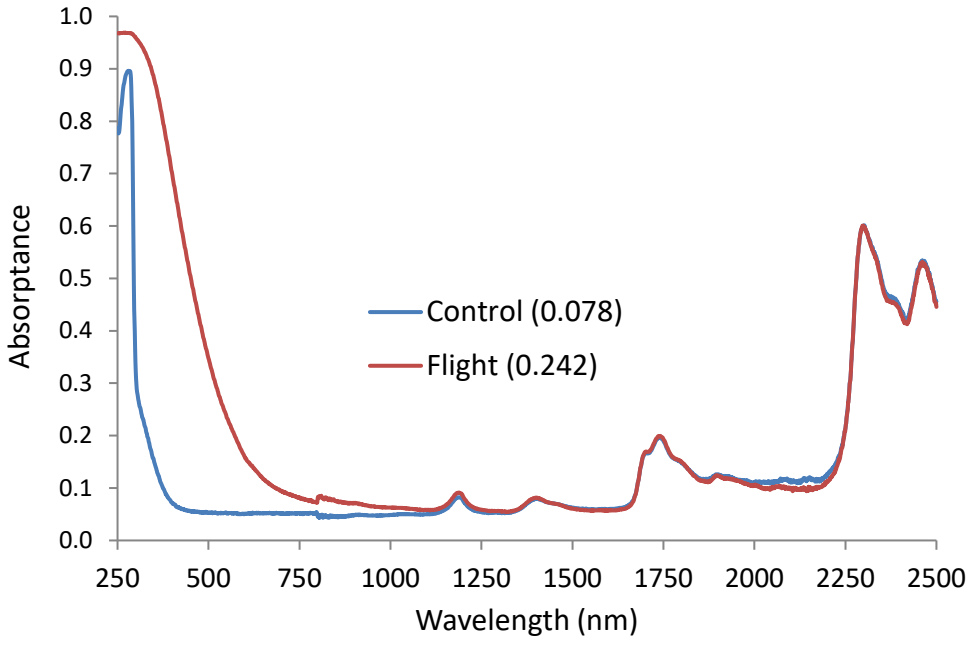


b.

*Figure 23. MISSE 7 Zenith Z-7 PVF: a). Post-flight photograph of the flight and control samples, and b). Absorptance curves for the flight (0.242) and control (0.078) samples (12 of 12 layers).*

Figure 24 shows the absorptance curves and post-flight images of Z-8, a set of 3 layers of Kapton H. This sample was flown to measure the AO fluence in the zenith direction. As can be seen in Figure 24b, the $\alpha_s$ change was relatively small (increase from 0.438 to 0.467 for all 3 layers). The Kapton H flight sample also displayed an unexplained jump in the spectra at 800 nm, similar to the ECTFE sample.

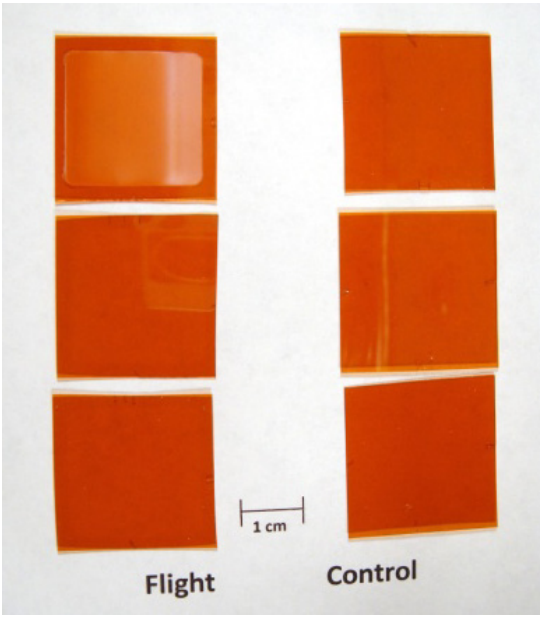


a.

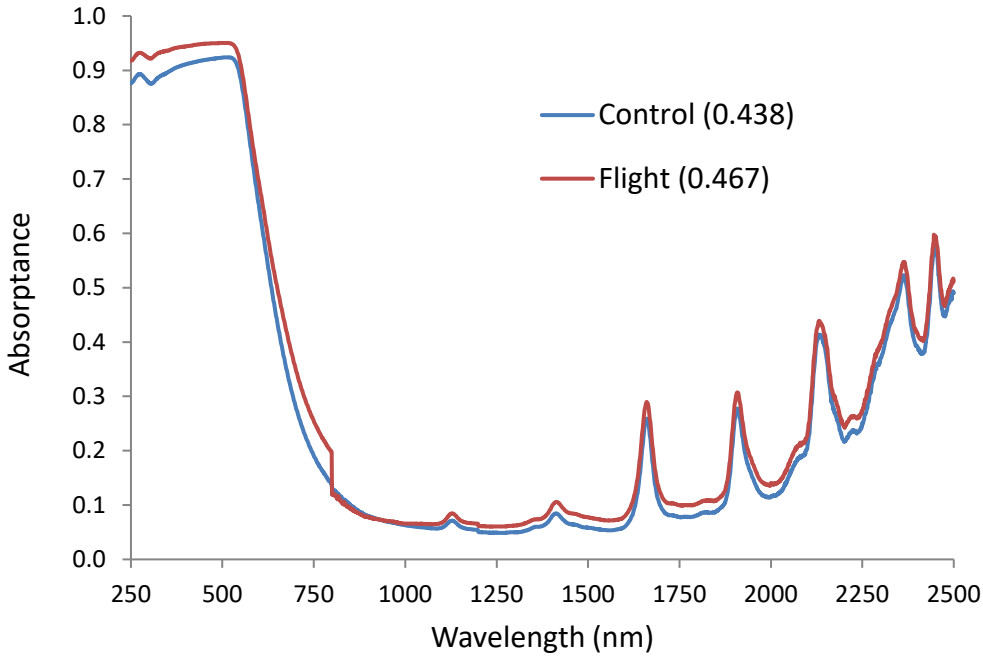


b.

*Figure 24. MISSE 7 Zenith Z-8 Kapton H: a). Post-flight photograph of the flight and control samples, and b). Absorptance curves for the flight (0.467) and control (0.438) samples (3 of 3 layers).*

Figures 25, 26, and 29 show the results for three FEP samples with different coatings: Al (back-surface coated), Ag (back-surface coated), and $Al_2O_3$ (front surface coated) respectively. The Al and Ag back-surface coated films are opaque with zero transmittance. Because the two back-surface coated FEP flight samples were significantly bowed, the diffuse and specular reflectance data is not reliable, and hence is not reported. Absorptance changes for the Al-FEP and Ag-FEP samples were similar at 0.061 and 0.052, respectively. It should be noted that the control Ag-FEP $\alpha_s$ is higher than typically reported. The $\alpha_s$ increase for the alumina coated FEP (0.041 to 0.066) was less than half (0.025) compared to the metal coated FEP samples.

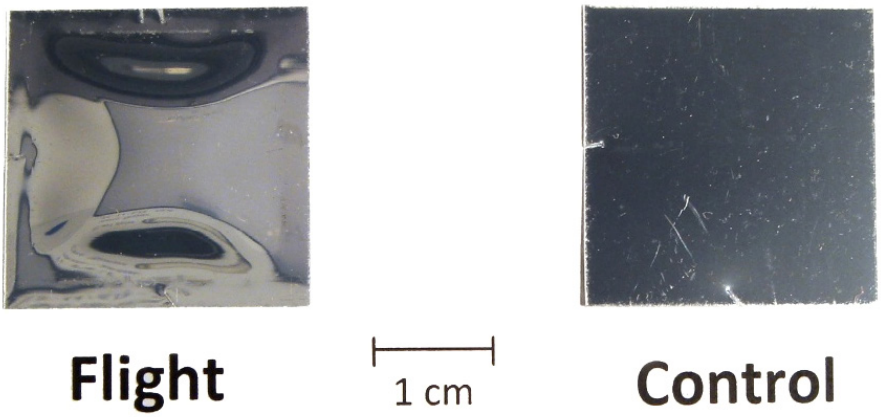


a.

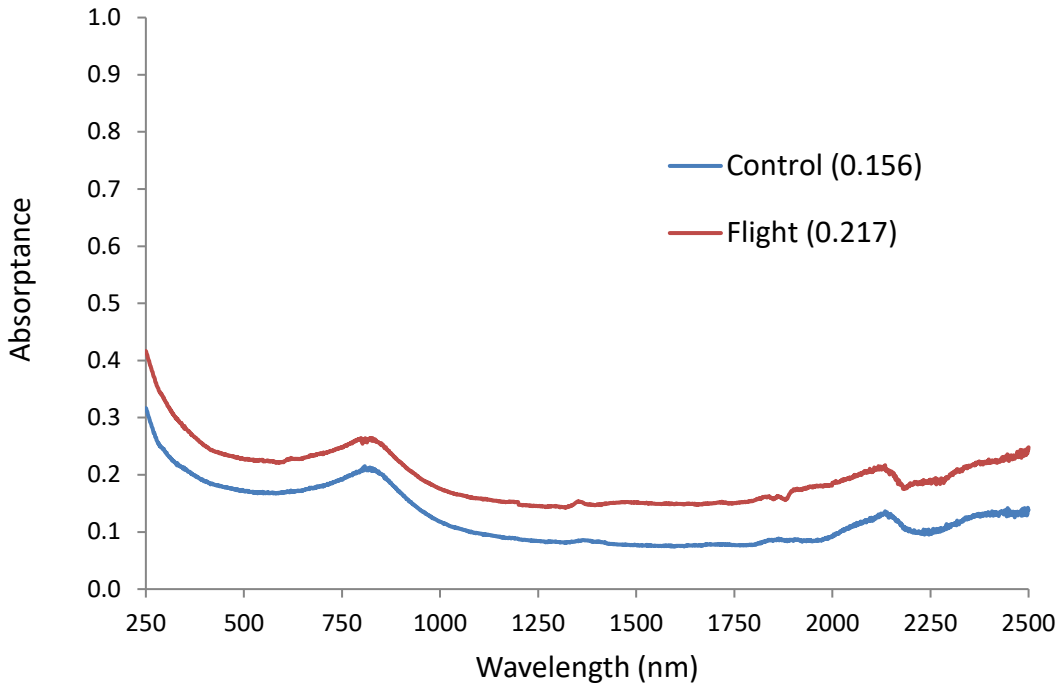


b.

*Figure 25. MISSE 7 Zenith Z-9 Al-FEP: a). Post-flight photograph of the flight and control samples, and b). Absorptance curves for the flight (0.217) and control (0.156) samples (1 layer).*

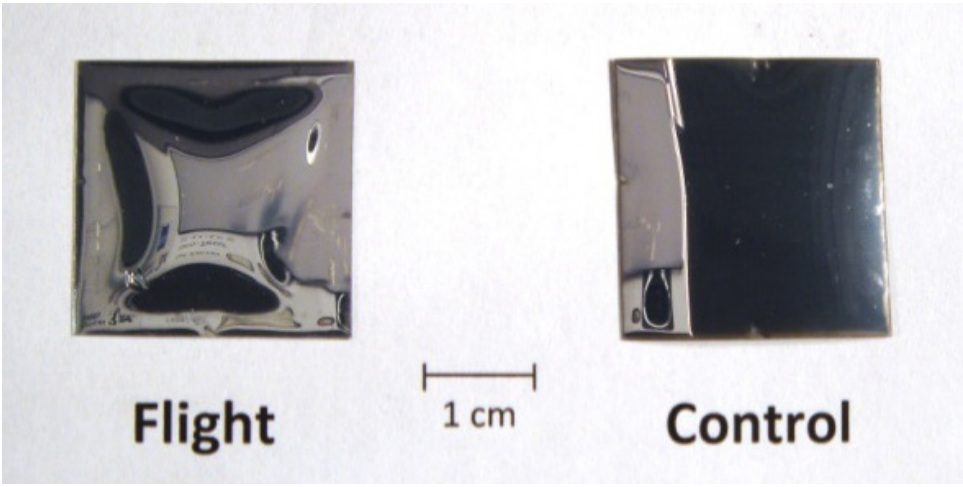


a.

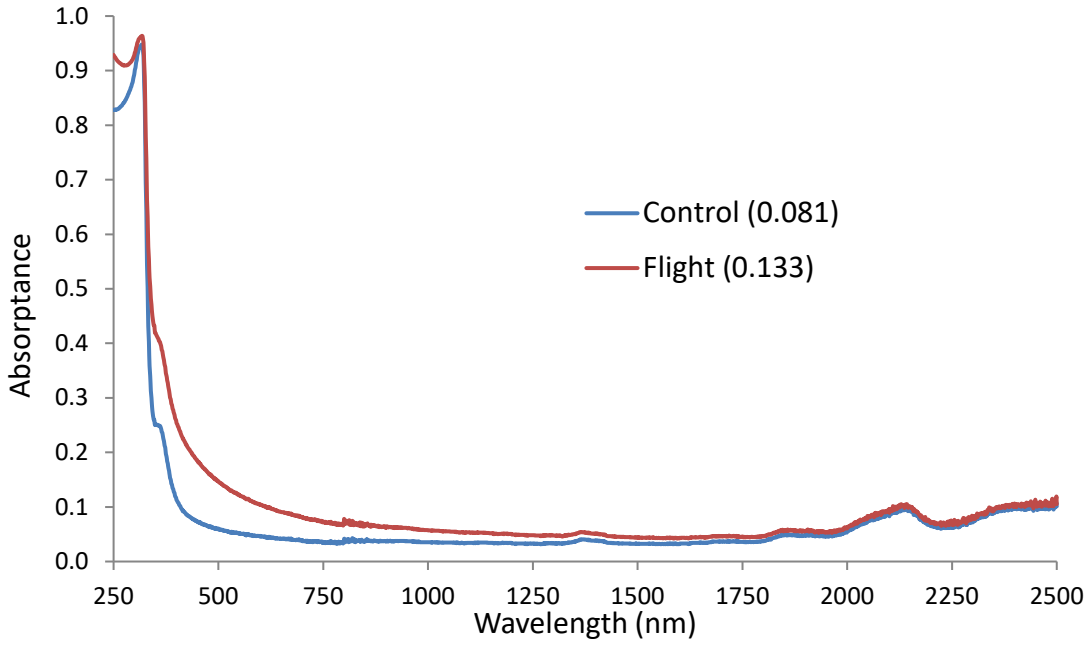


a.

*Figure 26. MISSE 7 Zenith Z-10 Ag-FEP: a). Post-flight photograph of the flight and control samples, and b). Absorptance curves for the flight (0.133) and control (0.081) samples (1 layer).*

Figure 27 shows a post-flight image and absorptance curves for the 8 layered PE (Z-11) sample. This material had rather high transmittance and a small $\Delta\alpha_s$ of 0.017 (0.071 to 0.088) for all 8 layers. The flight sample absorptance was lower than the control sample above 500 nm and higher than the control sample below 500 nm. A very small jump is seen in the flight sample spectra at 800 nm.

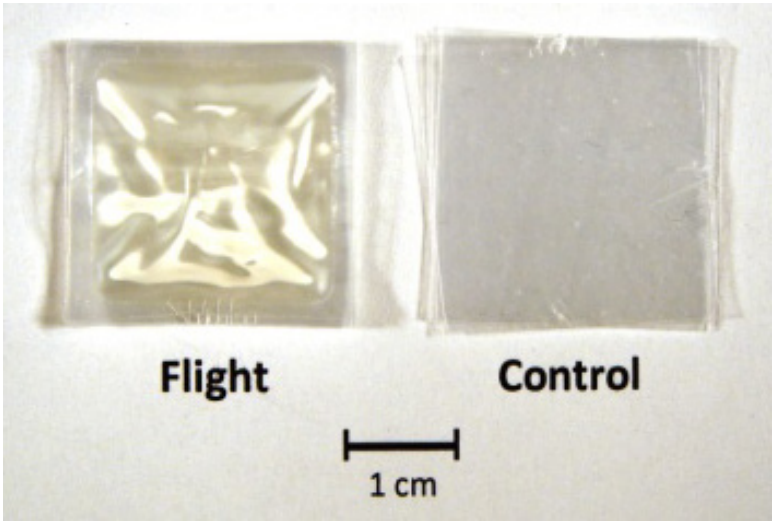


a.

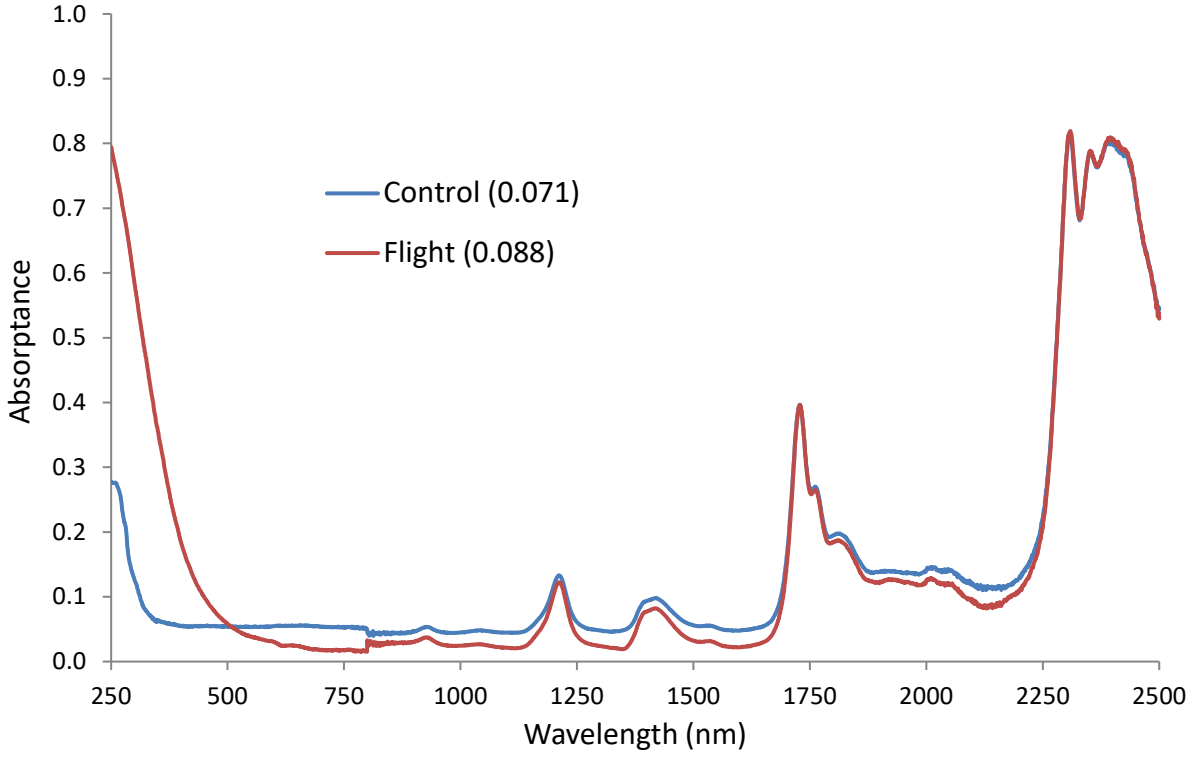


b.

*Figure 27. MISSE 7 Zenith Z-11 PE: a). Post-flight photograph of the flight and control samples, and b). Absorptance curves for the flight (0.088) and control (0.071) samples (8 of 8 layers).*

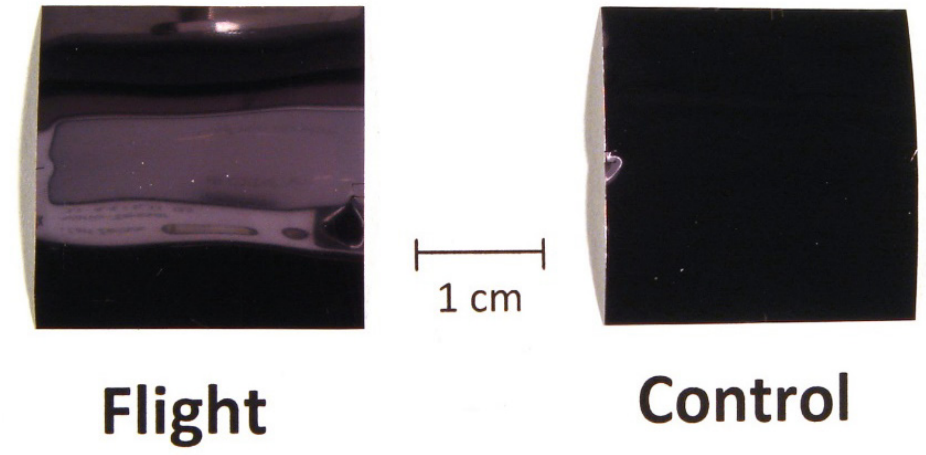


a.

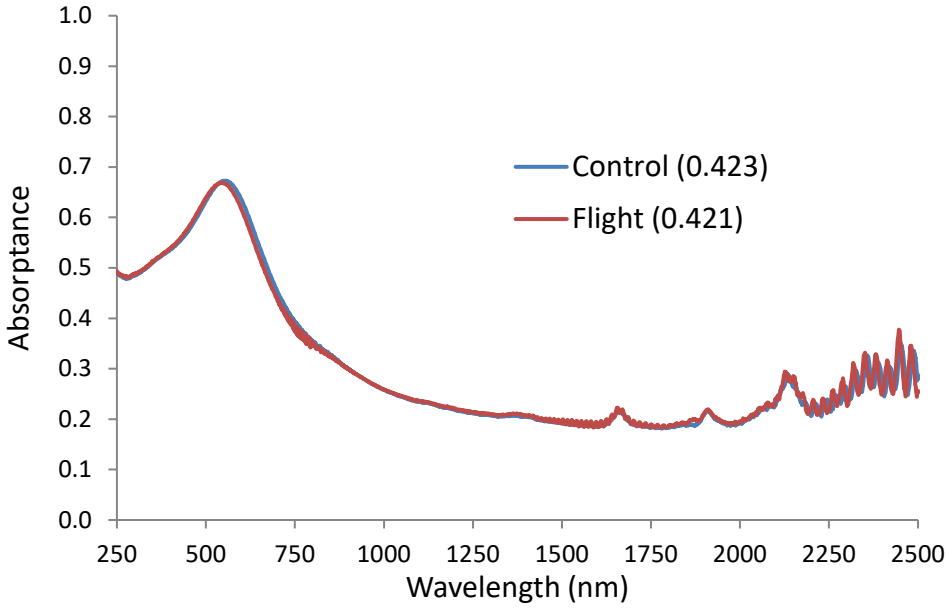


b.

*Figure 28. MISSE 7 Zenith Z-12 Si/Kapton E/Al: a). Post-flight photograph of the flight and control samples, and b). Absorptance curves for the flight (0.421) and control (0.423) samples (1 layer).*

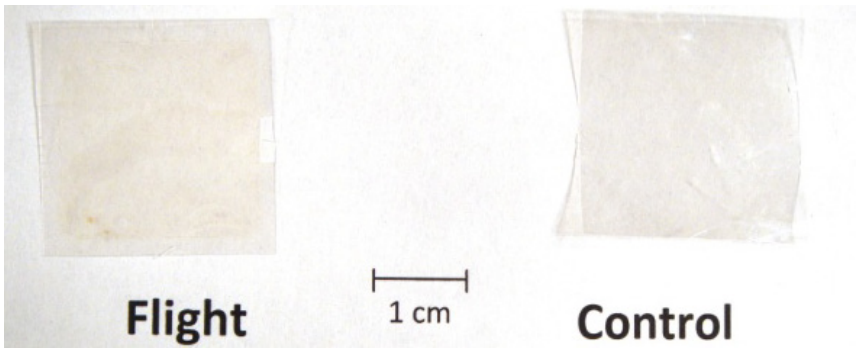


a.

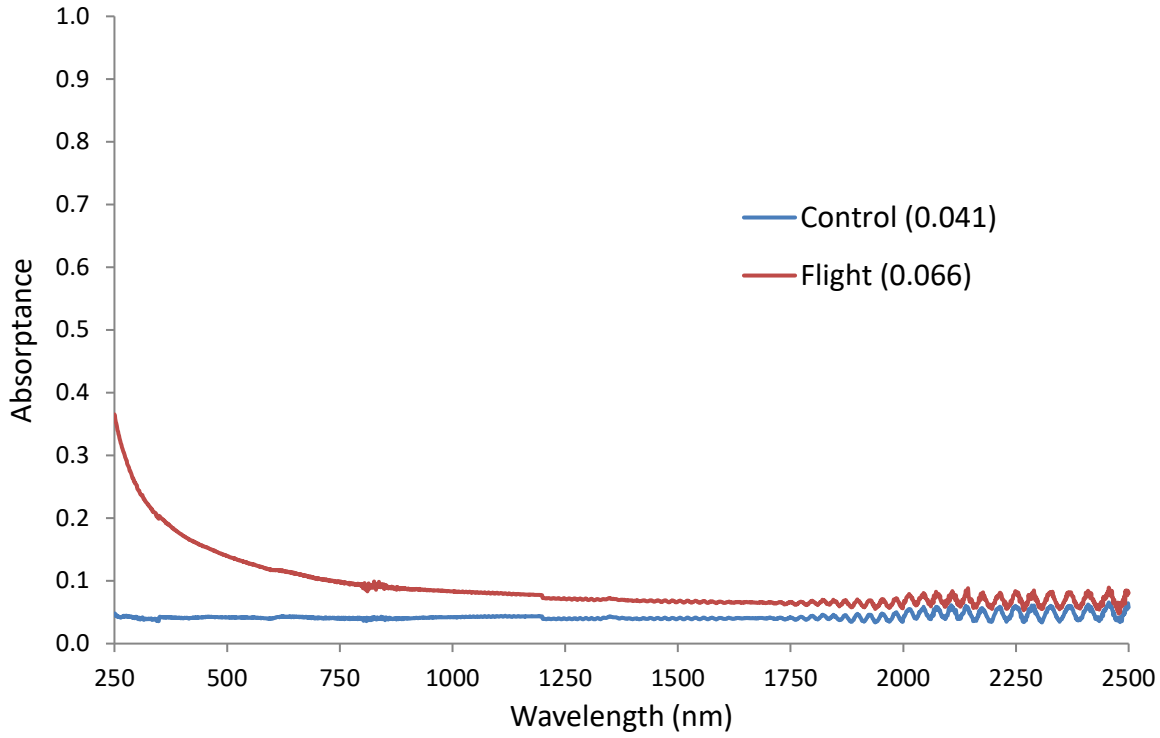


b.

*Figure 29. MISSE 7 Zenith Z-14 $Al_2O_3$/FEP: a). Post-flight photograph of the flight and control samples, and b). Absorptance curves for the flight (0.066) and control (0.041) samples (1 layer).*

Figure 30 shows a post-flight image of the flight sample (no control sample is shown) and absorptance curves for the 1 layer PP (E9) flight and control samples. This material behaved similar to other films such as ETFE (Z-4) which had very high total transmittance, moderately low $\Delta\alpha_s$, absorptance increases mainly in the lower UV wavelengths (<600 nm), and a color change from clear to brown. The absorptance of PP increased from 0.071 to 0.121. As seen in Figure 31, PVOH also appears to be similar to other highly transparent films, however PVOH transmittance was relatively low, and its $\Delta\alpha_s$ (from 0.079 to 0.203) rather high compared to films which appear to be similar such as ETFE. These differences are likely due in part to the number of layers scanned: 6 for PVOH, and 2 for ETFE. Slight browning occurred in the second and third layers of the 12 layer PVOH sample, as seen in Figure 31a where the top 3 layers are separated from the bottom 8 layers, contributing to transmittance decreases and absorptance increases.

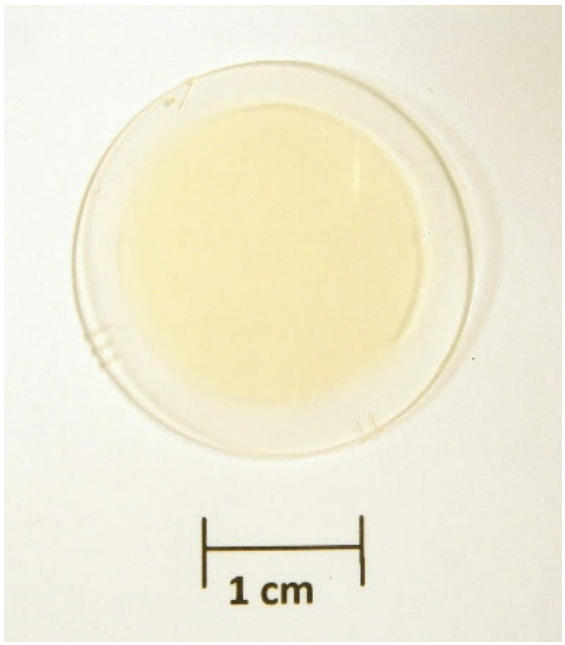


a.

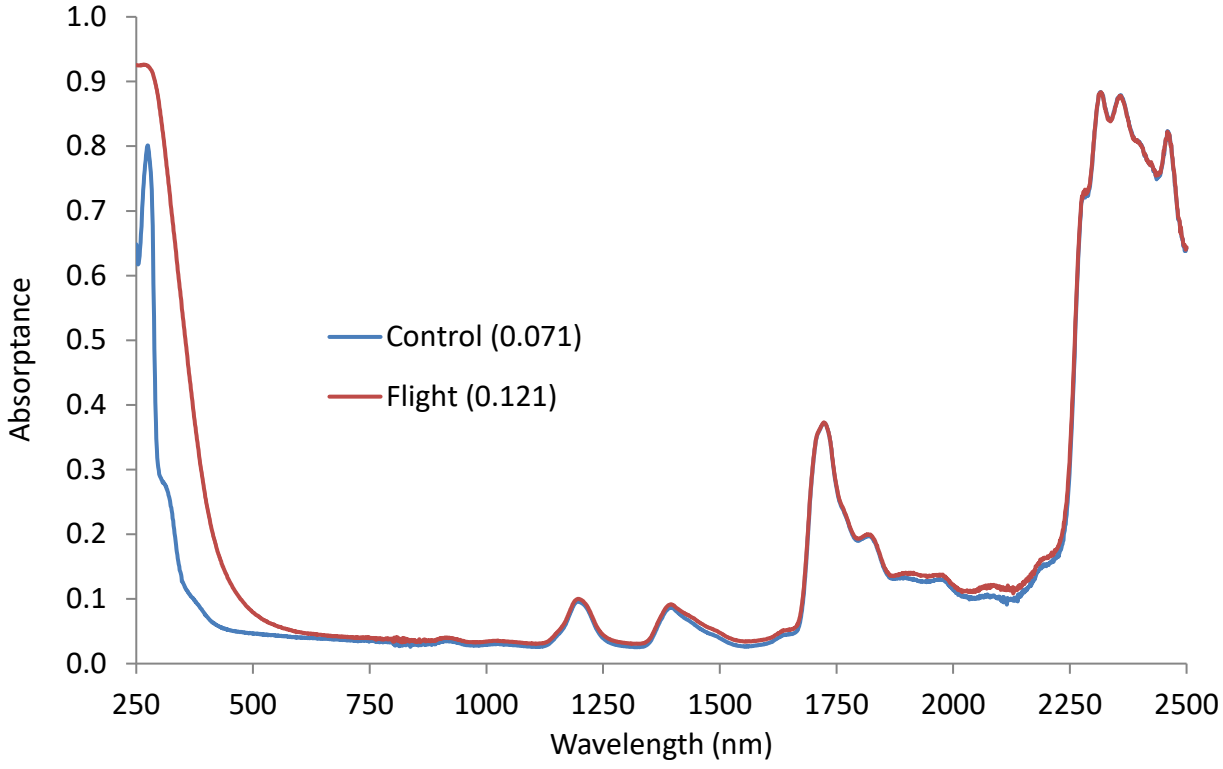


b.

*Figure 30. MISSE 7 Zenith E9 polypropylene: a). Post-flight photograph of the flight and control samples, and b). Absorptance curves for the flight (0.121) and control (0.071) samples (1 layer).*


a.

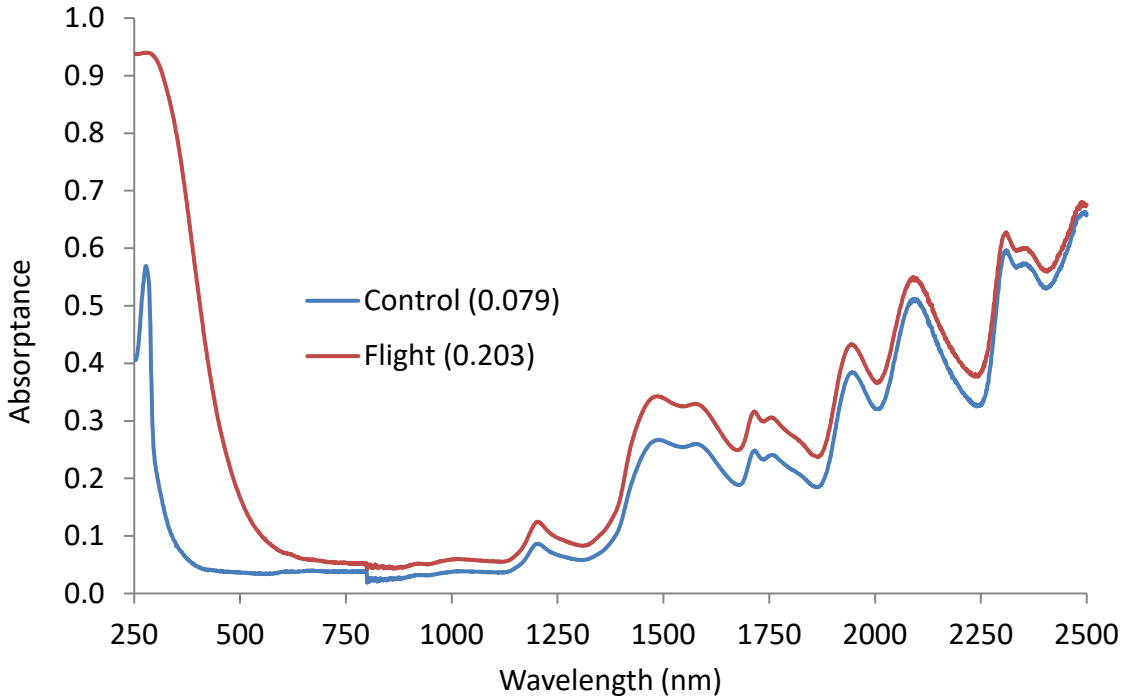


b.

*Figure 31. MISSE 7 Zenith P13-Z PVOH: a). Post-flight photograph of the flight and control samples, and b). Absorptance curves for the flight (0.203) and control (0.079) samples (6 of 12 layers).*

## MISSE 7 and MISSE 2 Comparison

Comparisons were made between changes in $\alpha_s$ and AO $E_y$ values between the MISSE 7 samples and similar materials flown as part of the MISSE 2 Polymers Erosion and Contamination Experiment (PEACE) ram experiment. Table 6 lists the flight orientation, space duration, and amount of AO fluence and solar radiation of the MISSE 7 ram and zenith samples, and the MISSE 2 ram samples. The MISSE 2 PEACE experiment did not include any zenith samples. MISSE 2 was flown in space for four years compared to MISSE 7 being flown in space for 1.5 years. The MISSE 2 ram samples received 2.6 times the amount of solar exposure (ESH) and 2 times the amount of AO fluence as MISSE 7 ram samples.

Table 7 lists and compares the changes in $\alpha_s$ and $E_y$ of MISSE 7 zenith polymers and their corresponding MISSE 2 ram polymers. These samples are compared, as 10 of the same polymers were flown in the MISSE 2 ram direction as in the MISSE 7 zenith direction. Even though the solar exposure and AO fluence for MISSE 2 are greater than those for the MISSE 7 zenith samples, the MISSE 7 zenith sample's solar/AO fluence ratio (272 x $10^{-19}$ ESH*cm$^2$/atom) is significantly greater than that of MISSE 2 (7.5 x $10^{-19}$ ESH*cm$^2$/atom). This means the MISSE 7 zenith samples were exposed to significantly longer hours of sunlight in relation to the dose of AO received compared to that experienced by MISSE 2. As can be seen in Table 7, the MISSE 7 zenith sample's $E_y$ values are all greater than the MISSE 2 sample's $E_y$ values with the exception of PVF (and Kapton H, used as an AO fluence witness sample) even though MISSE 2 was exposed to ~53.4X more AO exposure and 1.47X more solar ESH. However, the magnitude of solar exposure relative to AO exposure was 36.4 times higher for MISSE 7 than for MISSE 2. Thus, the erosion of the fluoropolymers appears to be significantly impacted by the higher dose of solar radiation compared to atomic oxygen exposure, and corresponding temperature effects. The impact of solar exposure on the erosion of fluoropolymers, such as Teflon FEP, in LEO has been observed previously.[12,16] On the other hand, except for ECTFE and PVF, the MISSE 2 ram samples had greater increases in $\alpha_s$ than the MISSE 7 zenith samples. This could be due to the longer total exposure to solar exposure and AO fluence resulting in greater changes in surface texture, coloration and thickness.

Table 8 lists changes in $\alpha_s$ and $E_y$ values of MISSE 7 ram polymers and similar materials flown on the MISSE 2 PEACE ram experiment. MISSE 2 samples, which were exposed to 2X the AO fluence and 2.6X the solar radiation, are found to have greater changes in $\alpha_s$ ($\Delta\alpha_s$). The $E_y$ of PP decreased slightly with the higher AO fluence and solar exposure on MISSE 2 as compared to MISSE 7, but the $\alpha_s$ of the PP increased significantly.

Table 6. MISSE 7 and 2 Environmental Exposure.

| MISSE Environmental Exposure | MISSE 7* (Ref. 1) | MISSE 7 (Ref. 1) | MISSE 2 (Ref. 15) |
|---|---|---|---|
| Flight Orientation | Ram | Zenith | Ram |
| Duration in space (years) | 1.5 | 1.5 | 4 |
| Solar Exposure (ESH) | 2400 | 4300 | 6300 |
| AO Fluence (atoms/cm$^2$) | $4.22\times10^{21}$ | $1.58\times10^{20}$ | $8.43\times10^{21}$ |
| Solar/AO F (E-19 ESH*cm$^2$/atom) | 5.69 | 272 | 7.5 |

*Full ram AO & ESH exposure

Table 7. Solar Absorptance and Erosion Data of MISSE 7 Zenith and MISSE 2 Ram Samples.

| | MISSE 7 Zenith | | MISSE 2 Ram | |
|---|---|---|---|---|
| **Material** | **Δ $\alpha_s$** | **$E_y$ ($cm^3$/atom)** (Ref. 1) | **Δ $\alpha_s$** (Ref. 13) | **$E_y$ ($cm^3$/atom)** (Ref. 15) |
| Chemfilm DF-100 (PTFE) | 0.001 | 9.19E-25 | 0.025 | 1.42E-25 |
| Teflon (FEP) | 0.001 | 9.74E-25 | 0.004 | 2.00E-25 |
| Kel-F (CTFE) | 0.021 | 2.15E-24 | 0.105 | 8.31E-25 |
| Tefzel ZM (ETFE) | 0.072 | 1.49E-24 | 0.095 | 9.61E-25 |
| Halar 300 (ECTFE) | 0.239 | 3.56E-24 | 0.116 | 1.79E-24 |
| Kynar 740 (PVDF) | 0.133 | 1.74E-24 | 0.153 | 1.29E-24 |
| Clear Tedlar (PVF) | 0.164 | 1.44E-24 | 0.096 | 3.19E-24 |
| Kapton H (PI) | 0.029 | 3.00E-24 (Ref. 6-9) | 0.077 | 3.00E-24 (Ref 6-9) |
| Polyethylene (PE) | 0.017 | 8.13E-24 | N/A | >3.74E-24 |
| Polypropylene (PP) | 0.05 | 2.77E-24 | 0.145 | 2.68E-24 |

Table 8. Solar Absorptance and Erosion Data of MISSE 7 Ram and MISSE 2 Ram Samples.

| | MISSE 7 Ram | | | | MISSE 2 Ram | | | |
|---|---|---|---|---|---|---|---|---|
| **Materials** | **AO Fluence (atoms/$cm^2$)** | **Solar Exposure (ESH)** | **Δ$\alpha_s$** | **$E_y$ ($cm^3$/atom)** (Ref. 1) | **AO Fluence (atoms/$cm^2$)** | **Solar Exposure (ESH)** | **Δ$\alpha_s$** (Ref. 13) | **$E_y$ ($cm^3$/atom)** (Ref. 15) |
| PP | 4.22E+21 | 2400 | 0.050 | 3.12E-24 | 8.43E+21 | 6300 | 0.145 | 2.68E-24 |
| Kapton H | 4.22E+21 | 2400 | 0.039 | 3.0E-24 (Ref. 6-9) | 8.43E+21 | 6300 | 0.077 | 3.0E-24 (Ref. 6-9) |
| White Tedlar | 4.22E+21 | 2400 | -0.070 | 1.48E-25 | 8.43E+21 | 6300 | -0.104 | 1.01E-25 |
| White Tedlar (0.5 mil Kapton H) | 3.79E+21 | <2400 | -0.078 | 1.54E-25 | N/A | N/A | N/A | N/A |
| White Tedlar (1 mil Kapton H) | 3.37E+21 | <2400 | -0.075 | 1.67E-25 | N/A | N/A | N/A | N/A |

As previously discussed, the $E_y$ for Kapton H was not measured for the MISSE 7 or MISSE 2 mission because the material was used as AO fluence monitor samples due to its well characterized LEO $E_y$. Kapton H experienced a relatively small increase in its $\alpha_s$ (0.038) due to the increased amount of solar exposure and atomic oxygen exposure for MISSE 2 as compared to MISSE 7.

White Tedlar consistently experienced a decrease in $E_y$ with increasing AO fluence. As discussed previously, AO and UV durable $TiO_2$ particles build up on the surface of white Tedlar with increasing AO fluence as the polymer matrix around the $TiO_2$ particles erodes away forming an AO and UV barrier if undisturbed. White Tedlar also became brighter with a decrease in $\alpha_s$ as its exposure to the space environment increased.

It was evaluated whether it was consistent that polymers with high $E_y$ values (>2.00E-24) had high changes in $\alpha_s$ (>0.05), while polymers with low $E_y$ (<2.00E-24) had lower changes in $\alpha_s$

(<0.05). This pattern was only consistent with a little more than half of the polymers, so it was concluded that there was not a conclusive trend.

## Summary and Conclusions

The Polymers Experiment and Zenith Polymers Experiment successfully flew on the exterior of the ISS as part of the MISSE 7 mission and were retrieved after 1.5 years of space exposure. The polymers were flown for LEO space environment durability analysis. Post-flight, the optical properties were obtained on seven ram and 15 zenith samples. In addition, solar absorptance changes and AO $E_y$ data were compared with similar samples exposed to the space environment for 4 years as part of the MISSE 2 mission.

The MISSE 7 ram $Al_2O_3$ slide (E13) had very little change in optical properties indicating very low on-orbit contamination in the ram flight direction. The $\Delta\alpha_s$ of Vespel (B7-9) was similarly unchanged. The $\alpha_s$ of all three white Tedlar samples decreased due to the space exposure; these negative $\Delta\alpha_s$ were caused by the buildup of AO and UV durable $TiO_2$ particles on the surface. These $TiO_2$ particles are left behind as the matrix of the film is eroded by AO. White Tedlar $\alpha_s$ stabilized with the lowest AO fluence of $3.37 \times 10^{21}$ atoms/cm$^2$. The $\alpha_s$ of ram oriented Kapton H (B7-8) and PP (E14) increased; the $E_y$ of these samples was also relatively high. Absorptance increases in Kapton H and PP were accompanied by texturing, color changes and mass loss.

MISSE 7 zenith samples received nearly double the amount of UV compared to MISSE 7 ram samples, and much less AO, 26X less. The MISSE 7 zenith samples atomic oxygen exposure was received at a grazing angle compared to ram samples. The optical properties of three materials flown in the zenith orientation were not significantly affected by the space exposure: PTFE (Z-1), FEP (Z-2) and Si/Kapton E/Al (Z-12). Three other materials: CTFE, PE, and $Al_2O_3$/FEP experienced small optical changes with zenith LEO exposure, all with $\Delta\alpha_s < 0.026$. Thus, the optical properties of these six materials are considered to have a high degree of space durability. Effects on the material, which include browning, texturing to a matte finish, and mass loss, combined to increase the absorptance of the remaining nine MISSE 7 zenith materials with $\Delta\alpha_s$ increases between 0.029 (for Kapton H) and 0.239 (for ECTFE). These moderate to high changes in absorptance may preclude the use of these materials without protection in LEO space applications.

MISSE 2 ram samples, which were exposed to 2.6X solar exposure ESH and 2X AO fluence as compared to the MISSE 7 ram samples, were found to have greater $\Delta\alpha_s$. MISSE 2 samples, which were exposed to greater total solar radiation and AO fluence, were darker and thus had greater $\Delta\alpha_s$ (with the exception of ECTFE and PVF). This is attributed to the greater amounts of threatening space environmental factors (solar exposure and AO fluence). In addition, the $E_y$ of the MISSE 7 zenith samples were greater than for the MISSE 2 ram samples (except PVF). This is attributed to solar radiation and corresponding temperature effects playing a significant role in the erosion of fluoropolymers.

In general, the solar absorptance of the flight samples was found to correlate to their change in color. The smaller the difference in color between the flight and control samples, the lower the change in the polymer's solar absorptance, while more vast changes in color translate to a greater change in solar absorptance. Therefore, it is possible to conclude that color comparison of flight

samples may be used as a simple method for roughly predicting the on-orbit optical durability of a polymer. This is a result of the peak in the AM0 solar spectrum residing in the wavelengths visible to the human eye (400 to 700 nm).

Understanding changes in the polymers' optical properties and $E_y$ values facilitates the selection of materials for spacecraft. Samples with high increases in $\alpha_s$ or with high $E_y$ should be avoided, or protected, when selecting materials for thermal control or other exterior spacecraft applications.

## References


1. de Groh, K. K., Banks, B. A., Yi, G. T., Haloua, A., Imka, E. C., Mitchell, G. G., Asmar, O. C., Leneghan, H. A. and Sechkar, E. A., "Erosion Results of the MISSE 7 Polymers Experiment and Zenith Polymers Experiment After 1.5 Years of Space Exposure," NASA TM-2016-219167, March 2017.
2. M. Nicolet and P. Mange, "The Dissociation of Oxygen in the High Atmosphere," J. Geophys Res (1954) Vol. 59, Issue 1, pp. 15-45.
3. 2000 ASTM Standard Extraterrestrial Spectrum Reference E-490-00 2000, Available at http://rrede.nrel.gov/solarsectra/AMO.
4. Dever, J.A., "Low Earth Orbital Atomic Oxygen and Ultraviolet Radiation Effects on Polymers," NASA TM 103711, February 1991.
5. de Groh, K. K, Banks, B. A., Dever, J. A., Jaworske, D. A., Miller, S. K., Sechkar, E.A., Panko, S. R., "NASA Glenn Research Center's Materials International Space Station Experiments (MISSE 1-7)," Prepared for the International Symposium on SM/MPAC and SEED Experiments, Epochal Tsukuba, Japan, March 10-11, 2008; also NASA TM-2008-215482.
6. Banks, B.A., Mirtich, M.J., Rutledge, S.K. and Swec, D.M. (1985). "Sputtered Coatings for Protection of Spacecraft Polymers," Thin Solid Films. Vol. 127, pp. 107–114.
7. Visentine, J.T., Leger, L.J., Kuminecz, J.F. and Spiker, I.K. (1985). STS-8 Atomic Oxygen Effects Experiment. Paper AIAA-85-0415 presented at the AIAA 23rd Aerospace Sciences Meeting. Reno, NV.
8. Koontz, S.L., Leger, L.J., Visentine, J.T., Hunton, D.E., Cross, J.B. and Hakes, C.L. (May-June 1995). "EOIM-III Mass Spectrometry and Polymer Chemistry: STS 46, July-August 1992," Journal of Spacecraft and Rockets. Vol. 32, No. 3, pp. 483–495.
9. Silverman, E.M. (August 1995). Space Environmental Effects on Spacecraft: LEO Materials Selection Guide. NASA CR-4661, Part 1. NASA MSFC: Huntsville, AL.
10. Hung, C. C., de Groh, K. K., Banks, B. A., "Optical and Scanning Electron Microscopy of the Materials International Space Station Experiment (MISSE) Spacecraft Silicone Experiment" August 2012; also NASA TM-2012-217678
11. PV Lighthouse website (accessed 3-14-18): https://www2.pvlighthouse.com.au/resources/courses/altermatt/The%20Solar%20Spectrum/The%20extraterrestrial%20(AM0)%20solar%20spectrum.aspx.

12. Banks, B. A., Simmons, J. C., de Groh, K. K., Miller, S. K., "The Effect of Ash and Inorganic Pigment Fill on the Atomic Oxygen Erosion of Polymers and Paints", Proceedings of the '12th Int. Symposium on Materials in the Space Environment (ISMSE 12)', Noordwijk, The Netherlands (ESA SP-705, March 2013).

13. Waters, D. W., de Groh, K. K., Banks, B. A., "Changes in Optical and Thermal Properties of the MISSE 2 PEACE Polymers and Spacecraft Silicones," September 15-18, 2009.

14. de Groh, K. K., Perry, B. A., Banks, B. A., Leneghan, H. A., Asmar, O. C. and Haloua, A., "Effect of 1.5 Years of Space Exposure on Tensile and Optical Properties of Spacecraft Polymers." Presentation given at the 2015 International Space Station Research and Development Conference (ISSRDC), Boston, MA, July 7-9, 2015.

15. de Groh, K. K., Banks, B. A., McCarthy, C. E., Rucker, R. N., Roberts, L. M. and Berger, L. A., "MISSE 2 PEACE Polymers Atomic Oxygen Erosion Experiment on the International Space Station," High Performance Polymers 20 (2008) 388-409.

16. de Groh, K. K. and Banks, B. A., "Atomic Oxygen Erosion Data from the MISSE 2-8 Missions," NASA/TM-2019-219982, May 2019.